THESIS APPROVAL

GRADUATE SCHOOL, KASETSART UNIVERSITY

Master of Science (Chemistry)

DEGREE

Chemistry	Chemistry
FIELD	**DEPARTMENT**

TITLE: Adsorption of Chromium (III) and Phenol by Activated Bamboo Charcoal (*Thyrsostachys siamensis* Gamble) Activated with Nitric Acid

NAME: Miss Chittraporn Chantasorn

THIS THESIS HAS BEEN ACCEPTED BY

THESIS ADVISOR

(Associate Professor Apisit Songsasen, Ph.D.)

DEPARTMENT HEAD

(Associate Professor Supa Hannongbua, Dr.rer.nat.)

APPROVED BY THE GRADUATE SCHOOL ON

DEAN

(Associate Professor Gunjana Theeragool, D.Agr.)

THESIS

ADSORPTION OF CHROMIUM (III) AND PHENOL BY ACTIVATED BAMBOO CHARCOAL (*THYRSOSTACHYS SIAMENSIS* GAMBLE) ACTIVATED WITH NITRIC ACID

CHITTRAPORN CHANTASORN

A Thesis Submitted in Partial Fulfillment of
the Requirements for the Degree of
Master of Science (Chemistry)
Graduate School, Kasetsart University
2012

Chittraporn Chantasorn 2012: Adsorption of Chromium (III) and Phenol by Activated Bamboo Charcoal (*Thyrsostachys siamensis* Gamble) Activated with Nitric Acid. Master of Science (Chemistry), Major Field: Chemistry, Department of Chemistry. Thesis Advisor: Associate Professor Apisit Songsasen, Ph.D. 112 pages.

Bamboo wood (*Thyrsostachys siamensis* Gamble) was carbonized at 450 ° C. The carbonized charcoals were then ground and sieve to less than 150 µm and activate with 70 % HNO_3 for 3 hours. The bamboo charcoal (BC) and bamboo activated charcoal (BAC) obtained were characterized by Fourier transform Infrared Spectrometry (FT-IR) and Scanning electron microscope (SEM). The present of broad peak in the range of 3,450 – 3,350 cm^{-1} was defined as O-H stretching vibration of hydroxyl group. The C-C stretching vibration of aromatic group can be observed in the range of 1,580 – 1,540 cm^{-1} and the band at 1,200-1,000 cm^{-1} was difficult to assigned because of the overlapping band. The weak absorption band can be observed at 880 – 650 cm^{-1} was attributed to C-H bending of aromatics or cyclic group.

The maximum Cr(III) removal efficiency of BC and BAC at optimum pH 4.0 (for both BC and BAC), were 92.61 ± 0.94% and 92.68 ± 0.87% and the maximum adsorption capacity were 1.01 mg/g and 1.98 mg/g respectively. The phenol values of BC and BAC for adsorption ability of phenol were 28.09±1.37 g/L and 19.35 ± 0.08 g/L, and the adsorption capacity were 0.19 mg/g and 0.26 mg/g respectively. The obtained specific surface area of BC and BAC were in the range of 5-53 m^2/g. Phenol value of BAC had significant difference from BC ($p \leq 0.05$; paired t-test) and the adsorption mechanism of phenol should be fitted with Freundlich isotherm model as considered from the correlation coefficient (R^2).

______________________________ ______________________________ ___ / ___ / ___

Student's signature Thesis Advisor's signature

ACKNOWLEDGEMENTS

I sincerely thank my advisor, Associate Professor Apisit Songsasen for his tremendous support and meticulous attention throughout the duration of my graduate study and research. I also wish to express my appreciation to my advisory committee, Dr. Boontana Wannalerse and Dr. Jirut Wattoom for their worthy suggestion and constructive criticism.

I would like to express my deep gratitude to the Center of Excellence for Innovation in Chemistry: Postgraduate Education and Research Program in Chemistry (PERCH-CIC) Science and Technology Postgraduate Education and Research Development Office (PERDO) for financial support and the Department of Chemistry, Faculty of Science, Kasetsart University for all research facilities.

Finally, I wish to thank my family and friends for their valuable advice, encouragement and understanding.

Chittraporn Chantasorn
August 2012

TABLE OF CONTENTS

LIST OF TABLES

Table **Page**

Appendix Table

LIST OF TABLES (Continued)

Appendix Table **Page**

LIST OF FIGURES

LIST OF FIGURES (Continued)

Figure **Page**

Appendix Figure

LIST OF ABBREVIATIONS

BAC = Bamboo Activated Charcoal
BC = Bamboo Charcoal
EAC = Extruded Activated Carbon
GAC = Granular Activated Carbon
PAC = Powder Activated Carbon
ASTM = American Society for Testing and Materials
AWWA = American Water Works Association
LD 50 = Median lethal dose
BET = Brunauer–Emmett –Teller
UV-Vis = UV-Vis Spectrophotometry
FT-IR = Fourier Transform Infrared Spectroscopy
T = Temperature
^{0}C = *Degree* Celsius
K = kelvin
ΔH_{ads} = heat of adsorption
g = gas
h = hour
P = pressure
P_s = saturation pressure
ml = milliliter
mm = millimeter
µm = micrometer
nm = nanometer
Å^2 = square angstrom
m^2 = Square meter
min^{-1} = per minute
ppm = part per million
mg/L = milligram per liter
mg/g = milligram per gram

LIST OF ABBREVIATIONS (Continued)

g/mol = gram per mol
%w/v = percentage weight by volume
cm^3/g = cubic centimeter per gram
m^2/g = square meter per gram
L/mg = liter per milligram
mg/m^2 = milligram per square meter
mL/min = milliliter per minute
rpm = rotation per minute

ADSORPTION OF CHROMIUM (III) AND PHENOL BY ACTIVATED BAMBOO CHARCOAL (*THYRSOSTACHYS SIAMENSIS* GAMBLE) ACTIVATED WITH NITRIC ACID

INTRODUCTION

1. Activated carbon

1.1 Definition of activated carbon

Activated carbon, also called activated charcoal or activated coal is a form of carbon that has been processed to make it extremely porous and thus to have a very large surface area available for adsorption or chemical reactions.

The word *activated* in the name is sometimes replaced with *active*. Due to its high degree of microporosity, just one gram of activated carbon has a surface area in excess of 500 m^2, as determined by nitrogen gas adsorption. Sufficient activation of useful applications may come solely from the high surface area, through further chemical treatment often enhances the adsorbing proteries of material.

Activated charcoal in its broadest sense includes a wide range of a processed amorphous carbon-based material. It is not truly an amorphous material but has a microcrystalline structure that starts to build up during the carbonization process. However, the activated carbon microcrystalline structure differs from that of graphite with respect to the interlayer spacing which is 0.335 nm in the case of graphite and ranges between 0.34 and 0.35 nm in activated carbon. The orientation of the microcrystallite layers is also different, being less ordered in activated carbon. The structures of activated carbon are shown in figure 1. Activated carbon is a fine black odorless and tasteless powder made from wood or other materials that have been processed to make it extremely porous and thus to have a very large surface area available for adsorption. One gram of activated carbon has a surface area of approximately 500 m^2 (or about 2 tennis courts) as determined typically by nitrogen gas adsorption (Bansal and Goyal, 2005). Activated carbon in the form of carbonized wood charcoal has been used for many centuries. The Egyptians used this charcoal about 1,500 BC as an adsorbent for medicinal purposes and also as a purifying agent. The ancient Hindus in India purified their drinking water by filtration through charcoal. The first industrial production of activated carbon started about 1900 for use in sugar refining industries. This activated carbon was prepared by the carbonization of a mixture of materials of vegetable origin in the presence of metal chlorides or by activation of the charred material by carbon dioxide (CO_2) or steam. Better quality gas-adsorbent carbon received attention during World War I, when they were used in gas masks for protection against hazardous gases and vapours.

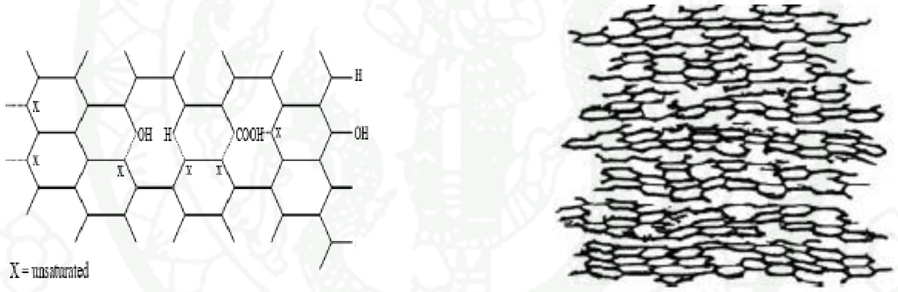

Source: Berl (1938)

Source: Tershkol (1969)

Source: Mattson and Mark (1971)

Source: Suzuki (1990)

Figure 1 The structures of activated carbon.

1.2 Classification

1.2.1 Powder activated carbon (PAC)

Traditionally, activated carbons are made in particular form as powder or fine granules which less than 1.0 mm in size with an averaged diameter between 0.15 to 0.25 mm. Thus they present a large surface to volume ratio with a small diffusion distance. PAC is made up of crushed or grounded carbon particles, 95-100% of which will pass through a designated mesh sieve or sieve. Granular activated carbon is defined as the activated carbon being retained on a 50 mesh sieve (0.297mm) and PAC as finer material, while ASTM classifies particle sizes corresponding to an 80 mesh sieve (0.177 mm) and smaller as PAC. PAC is generally used by directly adding to the other process unit, such as raw water in takes, rapid mix basins, clarifiers, and gravity filters.

1.2.2 Granular activated carbon (GAC)

Granular activated carbon is irregular shaped particles with sizes ranging from 0.2 to 5 mm. which has a relatively larger particle size compared to powdered activated carbon and consequently, presents a smaller external surface. Granulated carbon is used for water treatment, deodorization and separation of components of flow system. This type is used in both liquid and gas phase applications.

1.2.3 Extruded activated carbon (EAC)

Extruded activated carbon combines powdered activated carbon with a binder, which are fused together and extruded into a cylindrical shaped activated carbon block with diameters from 0.8 to 130 mm. These are mainly used for gas phase applications because of their low drop, high mechanical strength and low dust content.

1.2.4 Impregnated carbon

Porous carbons containing several types of inorganic impregnant such as iodine, silver, cation (Al, Mn, Zn, Fe, Li, Ca) have also been prepared for specific application in air pollution control especially in museums and galleries. Due to antimicrobial and antiseptic properties, silver loaded activated carbon is used as an adsorbent for purifications of domestic water. Drinking water can be obtained from natural water by treating the natural water with a mixture of activated carbon and flocculating agent $Al(OH)_3$. Impregnated carbons are also used for the adsorption of H_2S and thiols (mercaptans). Adsorption rates for H_2S (as high as 50% by weight) have been reported.

1.2.5 Polymer coated carbon

This is a process by which a porous carbon can be coated with a biocompatible polymer to give a smooth and permeable coat without blocking the pores. The resulting carbon is useful for hemoperfusion. Hemoperfusion is a treatment technique in which large volumes of the patient’s blood are passed over an adsorbent substance in order to remove toxic substances from the blood.

1.3 Utilities of activated carbon

Activated carbon, the common factor in hundreds of different applications just a grab from the numerous application : decolourisation of sugar and sweeteners, drinking water treatment, gold recovery, production of pharmaceuticals and fine chemical, catalytic processes, off gas treatment of waste incinerators, automotive vapour filters, colour/odour correction in wines and fruit juices, additive in liquour ice, etc.

In its applications, activated carbon represents a number of different functionalities:

Adsorption: the well-known mechanism, through chemisorption or physisorption (Van der Waals forces)

Reduction: e.g. removal of chlorine from water based on chemical reduction reactions.

Catalysis: Activated carbon can catalyzed a number of chemical convertions or used as a carrier for catalytic agents (e.g. precious metals).

Carrier of biomass: supported material in biological filters.

Carrier of chemicals: e.g. slow release applications colourant, activated carbon’s function in decolourizing.

1.4 The activation process of activation carbon

Activation process refers to the development of the adsorption properties of the carbon. It can be produced by one of the following processes.

1.4.1 Physical activation

The precursor is developed into activated carbon by using gases. It’s generally done by using one or the combination of the following processes.

Carbonization: Material with carbon content is pyrolyzed at the temperature in the range of 600-900 ^{0}C in the absence of air (usually in inert atmosphere with gases like argon or nitrogen).

Activation/Oxidization: Raw material or carbonized material is exposed to oxidizing atmosphere (carbon dioxide, oxygen or steam) at the temperature above 250^{0}C, usually in the range of 600-1200^{0}C.

1.4.2 Chemical activation

One of the key steps in the production of activated carbon is chemical activation through the impregnation of the raw material with chemical agents such as phosphoric acid, potassium hydroxide, zinc chloride. These activities improved the development of pore structure. Chemical activation is usually limit to woody precursors. Among the activating agent used for the production of activated carbon from carbonaceous materials, zinc chloride has been proven to be the one of the most effective impregnants. Zinc chloride acts as the hydration agent which is influencing the decomposition of carbonaceous material during the pyrolysis, thus restricting the formation of tar and increasing carbon yield. The degradation of cellulose material and aromatization of the carbon skeleton upon zinc chloride treatment results in the creation of pore structure. These pores are interstices left vacant upon the removal of zinc chloride from carbon matrix by intensive washing. The studied have clearly demonstrated that the amount of zinc chloride are used during the chemical activation significantly impacts the structure of the carbons. Chemical activation technique can be problematic in some cases, for example, zinc trace residues may remain in the end product. However, chemical activation is preferred over physical activation owing to the lower temperatures and short time needed for the activating material. Table 1 shows the examples of chemicals for the preparation of prepared activated carbon.

Table 1 Examples of chemicals for the preparation of activated carbon by chemical activation.

Acid	Base	Salt
Boric acid	Sodium hydroxide	Ferric chloride
(H_3BO_3)	(NaOH)	($FeCl_3$)
Phosphoric acid	Calcium hydroxide	Zinc chloride
(H_3PO_4)	($Ca(OH)_2$)	($ZnCl_2$)

Table 1 (Continued)

Acid	Base	Salt
Nitric acid (HNO_3)	Potassium hydroxide (KOH)	Potassium sulfide (K_2S)
Sulfuric acid (H_2SO_4)		Potassium thiocyanate (KSCN)
		Calcium phosphate ($Ca_3(PO_4)_2$)
		Calcium chloride ($CaCl_2$)

Source: Wikipedia (2012)

1.5 Activation with HNO_3

The formation of pores in activated carbon by nitric acid treatment was occurred when charcoal dissolved in hot nitric acid, a brown substance called “artificial tannin” was formed. However, concentrated nitric acid oxidized charcoal to CO_2 or metallic acid ($C_6(COOH)_6$) (Saxena, n.d.).

1.6 Porosity: definition

Based on experience of adsorption chemistry, the total porosity is classified into three groups. The origins and structure of porosities are shown below. IUPAC classifies porosities as follows:

Micropores width less than 2 nm
Mesopores width between 2 and 50 nm
Macropore width greather than 50 nm

It has been useful to classify micropores further into ulta- (<0.5 nm width) and super- (1.0-2.0 nm) micropores, these definitions being relevant when considering adsorption behavior. Microporosity are considered as being about the size of adsorbate molecules and accommodate one, two or three molecules. Mesoporosity is wider than microporoures. Macroporosity has little interest in the surface chemist. They are transport pores to the interior of the particles and are considered as external surface. Some activated charcoal contain all of these sizes of porosity deal with the botanical composition of the material. The pore size distribution is highly important for the practical application; the best fit depends upon the compounds of interest, the matrix (gas, liquid) and treatment condition. The desired pore structure of an activated carbon product is attained by combining the right raw material and activation conditions.

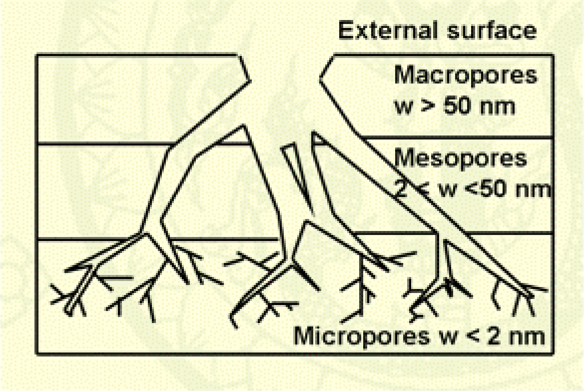

Figure 2 The classification of pores.

Source: Wikipedia (2012)

1.7 Chemical structure of the carbon surface

Besides the crystalline and porous structure, an activated carbon surface has its chemical structure. The adsorption capacity of activated carbon is determined by the porous structure. It is strongly influenced by the chemical structure of carbon surface. Graphites have a highly ordered crystalline surface, thus the adsorption capacity is determined mainly by the dispersion component of Van der Waals forces. But the random ordering of aromatic sheets in activated carbons causes a variation in the arrangement of electron clouds in the carbon skeleton. The results in the creation of unpaired electrons and incompletely saturated valences would undoubtedly influence the adsorption properties of activated carbons (Bansal and Goyal, 2005). Activated carbons are invariably deal with appreciable amounts of oxygen and hydrogen. In addition, it may be associated with heteroatoms such as sulfur, nitrogen, and halogens. These are derived from the starting material and become a part of the chemical structure as the result of imperfect carbonization, or they become chemically bonded to the surface during activation or subsequent treatments. It is also evidence that the carbon can adsorb certain molecular species such as amines, nitrobenzene, phenol, and several other cationic species.

1.8 Adsorption

Adsorption is the adhesion of molecule of gas, liquid, solid, or dissolved solids to a surface. This process create a film of *adsorbate* (the molecules or atoms being accumulated) on the surface of the *adsorbent.* It differs from *absorption,* in which a fluid permeated or be dissolved by a liquid or solid. The term sorption encompasses both processes, while desorption is the reverse process of adsorption.

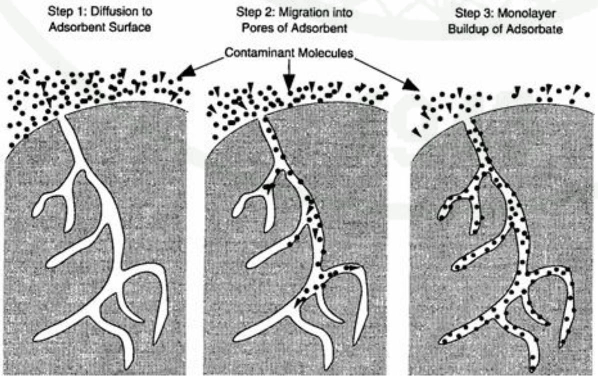

Figure 3 Adsorption process on the surface of adsorbate.

Source: pcd (2012)

1.9 Adsorption process

Adsorption arises as a result of the unsaturated and unbalanced molecular forces which are present on all of solid surface. When a solid surface contacted with a liquid or gas, the interaction between the fields of forces of the surface and that of the liquid or gas will occur. The solid surface tends to satisfy these residual forces by attracting and retaining on its surface the molecules, atom, or ion of the gas or liquid. The result shows that the concentration of the gas or liquid on the solid surface is more than in the bulk phase, even there is the nature of gas or vapor. The process by which this surface excess is caused is called adsorption. The adsorption characteristic into pores of adsorbent is also shown in Figure 4.

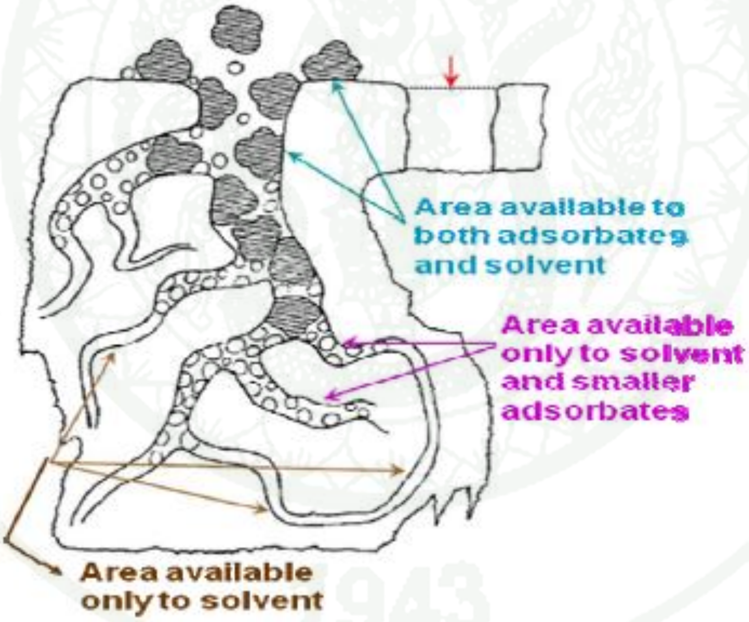

Figure 4 The adsorption characteristic into pores of adsorbent.

Source: Culp and Culp (1974)

Similar to surface tension, adsorption is a consequence of surface energy. In a bulk material, all the bonding requirements (e.g. ionic, covalent, or metallic) of the constituent atoms of the material are filled by other atoms in the material. However, atoms on the surface of the adsorbent are not wholly surrounded by other adsorbent atoms nd therefore can attract adsorbates. The exact nature of the bonding depends upon the details of species involved, but there are two different types of the adsorption processes.

1.10 Types of Adsorption

Forces of attraction exist between adsorbate and adsorbent. These forces of attraction are indicated by Vander waal forces of attraction which are weak forces due to chemical bond which are strong forces of attraction. On the basis type of forces of attraction existing between adsorbate and adsorbent, adsorption can be classified into two types: Physical Adsorption or Chemical Adsorption.

1.10.1 Physical Adsorption or Physisorption

When the force of attraction existing between adsorbate and adsorbent are weak Vander waal's forces, the process is called Physical Adsorption or Physisorption. It is also known as Vander waal's adsorption. Physical Adsorption takes place with formation of multilayer of adsorbate on adsorbent. It has low enthalpy of adsorption i.e. $\Delta H_{adsorption}$ is 20-40KJ/mol.

It takes place at low temperature below boiling point of adsorbate. As the temperature increases in, process of Physisorption decreases.

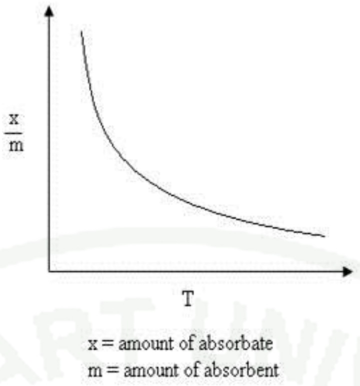

Figure 5 Physical adsorption vs. Temperature graph.

1.10.2 Chemical Adsorption or Chemisorption

When the force of attraction existing between adsorbate and adsorbent are chemical forces of attraction or chemical bond, the process is called Chemical Adsorption or Chemisorption. Chemisorption takes place with formation of unilayer of adsorbate on adsorbent. It has high enthalpy of adsorption.

i.e.

$$\Delta H_{adsorption} \text{ is } 200\text{-}400 KJ/mol.$$

It can take place at all temperature. With the increases in temperature, Chemisorption first increases and then decreases.

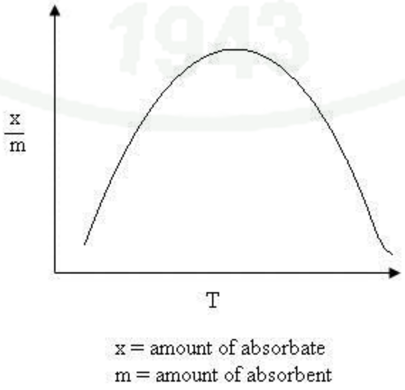

Figure 6 Chemical adsorption vs. Temperature graph

Table 2 Critical for distinguishing between chemisorption and physorption. (Bond, 1987)

Criteria	Chemisorption	Physisorption
Enthalpy of adsorption or heat od adsorption (ΔH_{ads})	>40 kJ/mol usually around 600-700 kJ/mol	0-40 kJ/mol
Activation energy, Ea	Usually small	Zero
Increasing tempurature	Irreversible	Reversible

The adsorption characteristics in solution phase between the adsorbent and adsorbate were explained by the adsorption isotherm models in general. Several models can be used to describe adsorption data. The two most frequency used for dilute solutions are Langmuir and Freundlich isotherms.

1.11 Adsorption isotherm

1.11.1 Basic adsorption isotherm

In the process of adsorption, adsorbate gets adsorbed on adsorbent.

$$\text{Adsorbate} + \text{Adsorbent} \underset{\text{desorption}}{\overset{\text{Adsorption}}{\rightleftharpoons}} \text{Adsorption}$$

$$A + B \rightleftharpoons AB$$

According to Le-Chatelier principle, the direction of equilibrium would shift in that direction where the stress can be relieved. In case of application of excess of pressure to the equilibrium system, the equilibrium will shift in the direction where the number of molecules decreases. Since number of molecules decreases in forward direction, with the increases in pressure, forward direction of equilibrium will be favored.

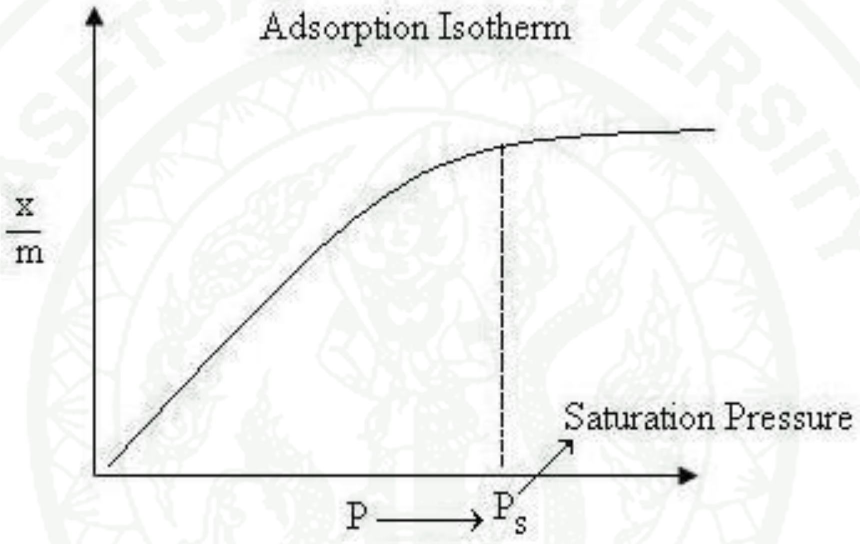

Figure 7 Basic Adsorption Isotherm.

From the graph in figure 7, it can be predict that after saturation pressure P_s, adsorption does not occur anymore. This can be explained by the fact that there are limited numbers of vacancies on the surface of the adsorbent. At high pressure a stage is reached when all the sites are occupied and further increase in pressure does not cause any difference in adsorption process. At high pressure, Adsorption is independent of pressure.

1.11.2 Langmuir adsorption isotherm

In 1916, Langmuir proposed another adsorption isotherm knows as Langmuir Adsorption Isotherm. This isotherm was based on different assumptions one of which is that dynamic equilibrium exists between adsorbed gaseous molecules and the free gaseous molecules.

$$\mathrm{A\,(g) + B\,(s)} \underset{\text{Desorption}}{\overset{\text{Adsorption}}{\rightleftharpoons}} \mathrm{AB}$$

Where A(g) is unadsorbed gaseous molecules, B(s) is unoccupied surface and AB is adsorbed molecule.

Based on this theory, Langmuir derived Langmuir Equation which depicted a relationship between the number of active sites of the surface undergoing adsorption and pressure.

$$q_e = \frac{Q_o b C_e}{(1+bC_e)} \quad \text{(Nonlinear form)} \quad (1)$$

Where;

C_e is the equilibrium concentration of the adsorbate (mg/L)

q_e is the amount of adsorbate adsorbed per unit mass of adsorbent (mg/g)

Q_o is the maximum surface coverage (formation of monolayer) of sorbent (mg/g)

b is the adsorption energy constant of Langmuir adsorption isotherm (L/mg) $b \ \alpha \ e^{(\Delta H/RT)})$

Equation (1) is usually linearlized by inversion to obtain the following from

$$\frac{C_e}{q_e} = \frac{1}{Q_0 b} + \frac{C_e}{Q_0} \quad \text{(Linear form)} \quad (2)$$

Many researchers have usually used equation (2) to analyze batch equilibrium data by plotting C_e /q_e versus C_e which yields a linear if data conform to the Lamgmuir isotherm.

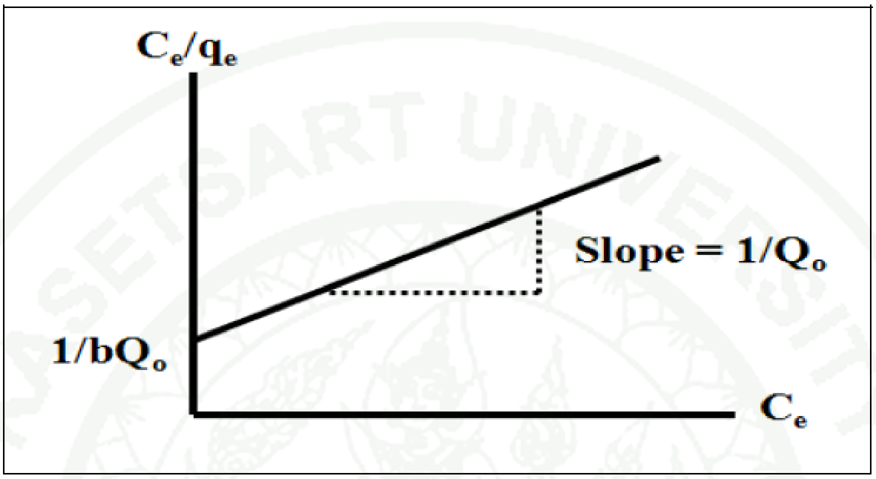

Figure 8 The Langmuir isotherm plots of C_e/ q_e versus C_e for adsorption.

Source: Cheremisinoff and Morresi (1987)

Once b is considered, this parameter can be rewritten as

$$b = b'e^{(\Delta Hads/RT)} \qquad (3)$$

Where ΔH_{ads} is enthalpy or heat of adsorption, R is the universal gas constant, T is the temperature in Kelvin and b' is pre-exponential factor constant. The heat of adsorption (ΔH_{ads}) can be determined from slope of the observed linearity from the plot of ln b (or log) versus 1/T that leads to heat process involved in adsorption of monolayer coverage.

When the molecule adsorbs on the surface of activated carbon based on the Langmuir isotherm, the specific surface area can be calculated as follows (Chongrak et al., 1998 and Itodo et al., 2010).

$$S = \frac{Q_o}{MW}\ x\ N\ x\ a \tag{4}$$

Where;

S is the specific surface area (m^2/g)

Q_o is the the maximum surface coverage (formation of monolayer) of sorbent (mg/g)

MW is the molecular weight (g/mol)

N is the Avogadro number (6.02×10^{23} molecule/mol)

a is the cross sectional area of adsorbate ($Å^2$)

1.11.2.1 Assumptions of Langmuir isotherm

Langmuir proposed his theory by making following assumptions.

a) Fixed number of vacant or adsorption sites are available on the surface of solid.

b) All vacant sites are of equal size and shape on the surface of solid.

c) Each site can hold maximum of one gaseous molecule and a constant amount of heat energy is released during this process.

d) Dynamic equilibrium exists between adsorbed gaseous molecules and free gaseous molecules.

e) Adsorption is monolayer or unilayer.

$$A\ (g) + B\ (s) \underset{\text{Desorption}}{\overset{\text{Adsorption}}{\rightleftharpoons}} AB$$

Where A(g) is unadsorbed gaseous molecules, B(s) is unoccupied surface and AB is adsorbed molecule.

1.11.2.2 Limitation of Langmuir adsorption equation.

a) The adsorbed gas has to behave ideally in the vapor phase. This condition can be fulfilled at low pressure conditions only. Thus Langmuir equation is valid under low pressure only.

b) Langmuir equation assumes that adsorption is monolayer. But, monolayer formation is possible only under low pressure condition. Under high pressure condition the assumption breaks down as gas molecules attract more and more molecules towards each other. BET theory proposed by Brunauer, Emmett and Teller explained more realistic multilayer adsorption process.

c) Another assumption was that all thesite on the solid surface are equal in size and shape and have equal affinity for adsorbate molecule i.e. the surface of solid if homogeneous. But we all know that in real solid surfaces are heterogeneous.

d) Langmuir equation assumed that molecules do not interact with each other. This is impossible as weak force of attraction exists even between molecules of same type.

e) The adsorbed molecules has to be localized i.e. decrease in randomness is zero ($\Delta S=0$). This is not possible because on adsorption liquefaction of gases taking place, which results into decrease in randomness but the value is not zero.

From above it can conclude that, Langmuir equation is valid under low pressure conditions.

1.11.3 Freundlich adsorption isotherm

Freundlich proposed another adsorption isotherm known as Freundlich adsorption isotherm or Freundlich adsorption equation or simply Freundlich isotherm. The Freundlich adsorption equation is perhaps the most widely used for the description of adsorption in aqueous systems. The Freundlich equation is of the form

$$q_e = k_F C_e^{\frac{1}{n}} \quad \text{(Nonlinear form)} \qquad (5)$$

Where;
q_e is the amount adsorbed at equilibrium (mg/g)
C_e is the equilibrium concentration of the adsorbate (mg/L)
k_F is the Freundlich isotherm constant related to adsorption capacity $((\mathrm{mg}^{-1})(\mathrm{mg}^{-1})^{1/n})$
n is the Freundlich isotherm constant related to adsorption intensity

The logarithm of equation (4) given below is usually used to fit data as

$$log q_e = log k_F + \frac{1}{2} log C_e \quad \text{(linear form)} \quad (6)$$

The above equation is comparable with equation of straight line, y = mx + c where, m represents slope of the line and c represents intercept on y axis.

Plotting a graph between log q_e and log C_e we will get a straight line with value of slope equal to n and log k_F as y-axis intercept. The slope 1/n ranging between 0 and 1 is a measure of adsorption intensity or surface heterogeneity, becoming more heterogeneous as its value closer to zero. A value for 1/n below one indicates a normal Langmuir isotherm (Type I Adsorption Isotherm) while 1/n above one is indicative of cooperative adsorption. The Freundlich isotherm plot of log q_e versus log C_e for the adsorption is shown in figure 9.

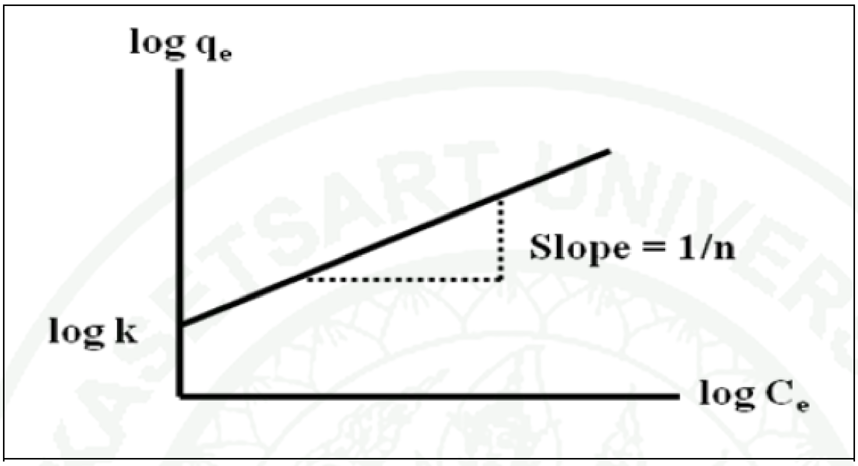

Figure 9 The Freundlich isotherm plots of log q_e versus log C_e for the adsorption.

Source: Cheremisinoff and Morresi (1987)

1.10.3.1 Limitation of Freundlich adsorption isotherm

Experimentally it was determined that extent of adsorption varies directly with pressure till saturation pressure P_S is reached. Beyond that point rate of adsorption saturates even after applying higher pressure. Thus Freundlich Adsorption Isotherm failed at higher pressure.

1.12 Type of Adsorption Isotherm

Five different types of adsorption isotherm and their characteristics are explained below.

1.12.1 Type I Adsorption Isotherm

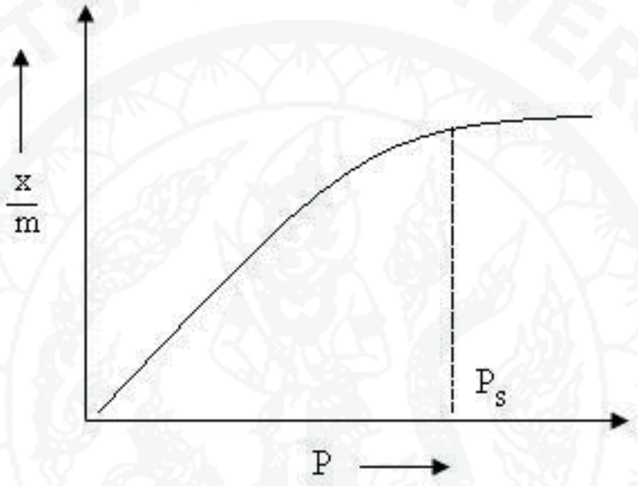

Figure 10 Type I Adsorption Isotherm

a) The above graph depicts Monolayer adsorption.

b) This graph can be easily explained using Langmuir Adsorption Isotherm.

c) If BET equation, when $P/P^0 << 1$ and $c >> 1$, then it leads to monolayer formation and Type I Adsorption Isotherm is obtained.

d) Examples of Type-I adsorption are Adsorption of Nitrogen (N_2) or Hydrogen (H_2) on charcoal at temperature near to -180 ^{0}C.

1.12.2 Type II Adsorption Isotherm

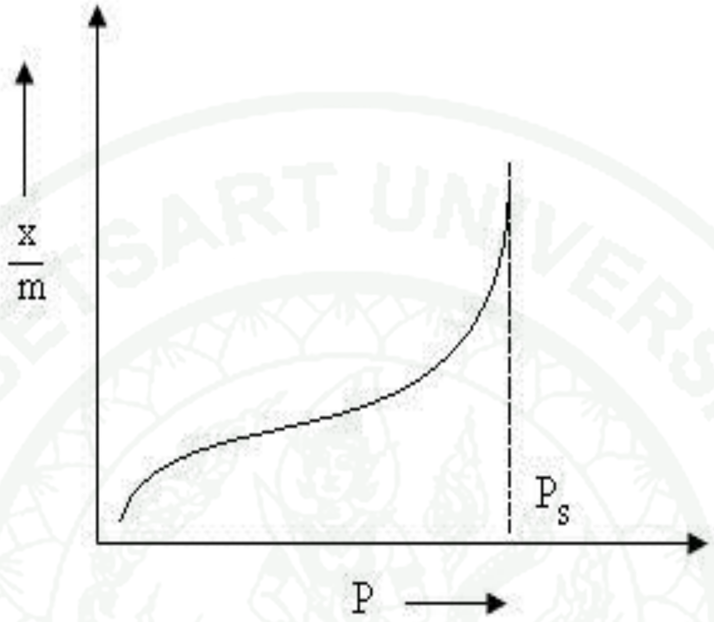

Figure 11 Type II Adsorption Isotherm.

a) Type II Adsorption Isotherm shows large deviation from Langmuir model of adsorption.

b) The intermediate flat region in the isotherm corresponds to monolayer formation.

c) In BET equation, value of C has to be very large in comparison to 1.

d) $\Delta H^0_{desl} > \Delta H^0_{vapl}$

e) Examples of Type-II adsorption are Nitrogen (N_2 (g)) adsorbed at -195 ^{0}C on Iron (Fe) catalyst and Nitrogen (N_2 (g)) adsorbed at -195 ^{0}C on silica gel.

1.12.3 Type III Adsorption Isotherm

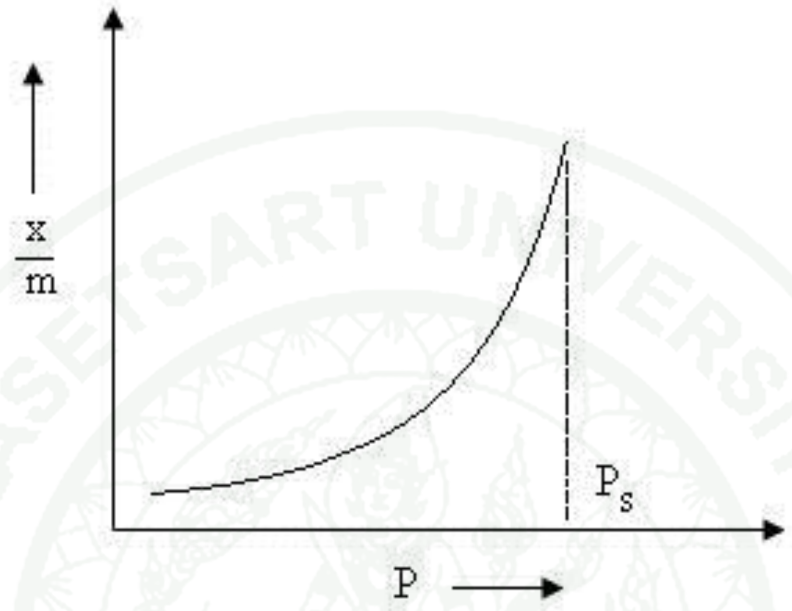

Figure 12 Type III Adsorption Isotherm.

a) Type III Adsorption Isotherm also shows large deviation from Langmuir model.
b) In BET equation value if C <<< 1 Type III Adsorption Isotherm obtained.
c) This isotherm explains the formation of multilayer.
d) There is no flattish portion in the curve which indicates that monolayer formation is missing.
e) Examples of Type III Adsorption Isotherm are Bromine (Br_2) at 79 ^{0}C on silica gel or Iodine (I_2) at 79 ^{0}C on silica gel.

1.12.4 Type IV Adsorption Isotherm

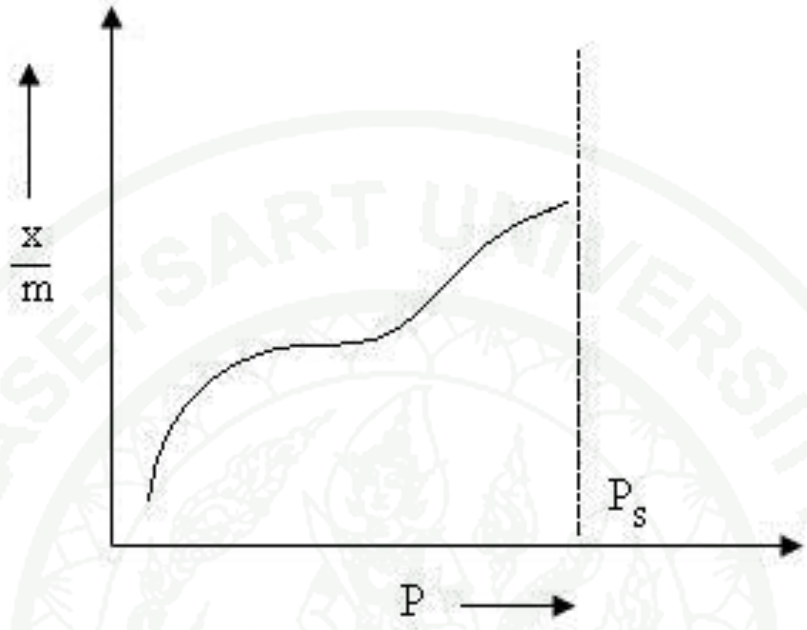

Figure 13 Type IV Adsorption Isotherm.

a) At lower pressure region of graph is quite similar to Type II. This explains formation of monolayer followed by multilayer.
b) The saturation level reaches at a pressure below the saturation vapor pressure. This can be explained on the basis of a possibility of gases getting condensed in the tiny capillary pores of adsorbent at pressure below the saturation pressure (P_S) of the gas.
c) Examples of Type IV Adsorption Isotherm are of adsorption of Benzene on Iron Oxide (Fe_2O_3) at 50 ^{0}C and adsorption of Benzene on silica gel at 50 ^{0}C.

1.12.5 Type V Adsorption Isotherm

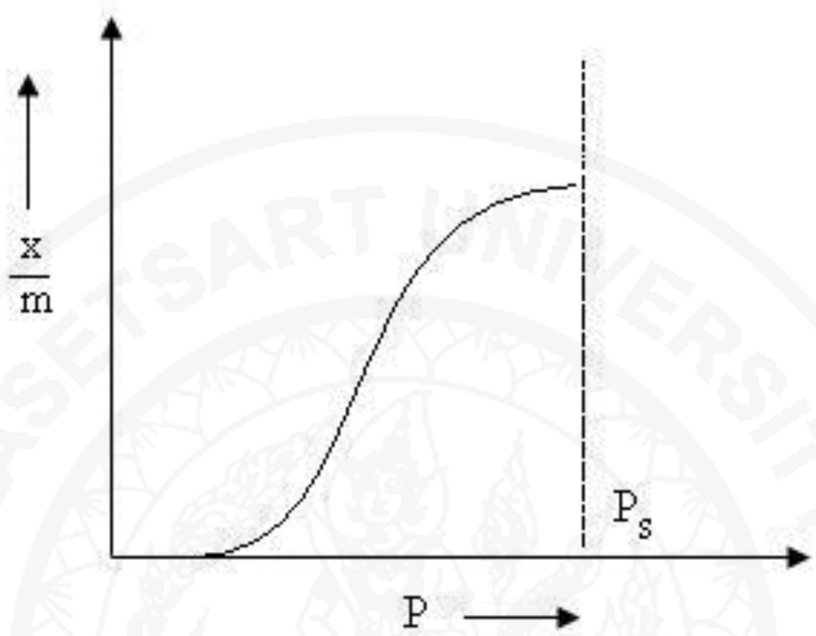

Figure 14 Type V Adsorption Isotherm.

a) Explanation of Type V graph is similar to Type IV.
b) Example of Type V Adsorption Isotherm is adsorption of Water (vapors) at 100 ^{0}C on charcoal.
c) Type IV and V shows phenomenon of capillary condensation of gas.

2. Bamboo

Bamboo is a group of woody perennial evergreen, except for certain temperate species, plants in the true grass family Poaceae, subfamily Bambusoideae, and tribe Bambuseae. Bamboo is the fastest growing woody plants in the world. Their growth rate (up to 60 centimeters/day) is upon a unique rhizome-dependent system, but is highly dependent on local soil and climate conditions. They are of economic and high cultural significance in East Asia and South East Asia which used extensively in gardens, as a building material, and as a food source.

2.1 *Thyrsostachys siamensis* Gamble

Familia: *Poaceae*
Subfamilia: *Bambusoideae*
Genus: *Thyrsostachys*
Species: *Thyrsostachys siamensis*
Common name: phairuak (Thai), monastery bamboo (English), umbrella-handled bamboo (English), shamudake (Japanease)

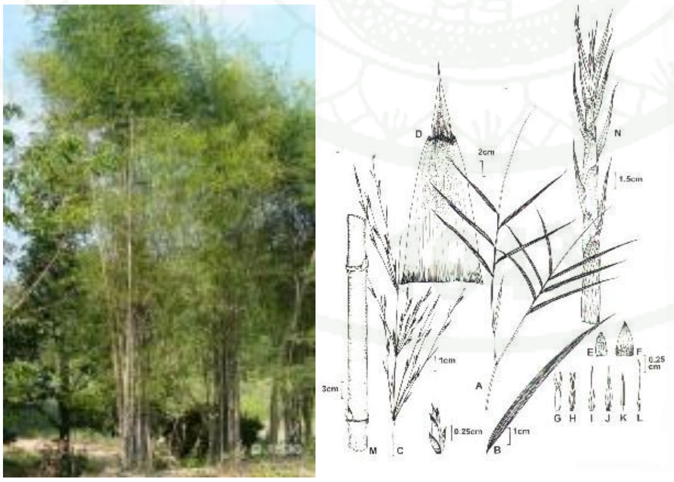

A - leafy branch; B - leaf;
C - flowering branch; D - culm-sheath;
E & F - empty glumes;
G & H - paleas of lower flower;
I & J - paleas of upper flow
K - stamen; L - pistil;
M - a portion of culm;
N - new shoot.

Figure 15 The image of *Thyrsostachys siamensis* Gamble.

Source: jircas (2012)., inbar (2012)

Culms; 8-10 m high and 4-5 cm diameter, straight, thick-walled, usually covered with the persistent culm-sheaths; internodes 20-30 cm long, green.

Culm-sheaths; 20-25 cm long, 10-20 cm broad, covered with fine white pubescence on the back, attenuate into a 3.5-4 cm broad, truncate top; ligule 2 mm high, narrow, slightly or irregularly toothed, finely ciliate; auricles short, triangular; blade
10-13 cm long, erect, narrowly triangular, edges incurved. In young shoots, blades tapering at the base, linear-lanceolate, sheath long with brown hairy margin.

Leaves; 8-15 cm long and 0.8-1.2 cm broad, narrow, linear, glabrous, short-stalked.

The chemical composition of culms; holocellulose 68%, lignin 24%, pentosans 7%, ash 2%, solibility in hot water 5.7% and in alcohol-benzene 6.1%.

Nutrition; In 100 g edible portion of bamboo shoot consists of water 89.5 g, protein 3.8 g, fat 0.3 g, carbohydrate 4.5 g, fibre 0.7 g, ash 1.0 g, Ca 12.8 mg, Fe 40.2 mg, P 0.2 mg, vitamin B1 0.01 mg, vitamin B2 0.09 mg and traces of vitamins A and C. The energy value is about 140 kJ/100 g.

3. Chromium

3.1 Physical and chemical properties

Chromium is a steel-gray luminous metallic element, atomic number 24, and its physicochemical properties include atomic weight, 51.996; specific gravity, 7.20; melting point, 1,900°C and boiling point, 2,642°C. Chromium metal reacts with diluted hydrochloric acid and sulfuric acid, but not with nitric acid. This metal has a valency of 0, II, III, V or VI. Elemental chromium (valency 0) which does not be occured naturally. The majority of chromium in nature is Cr(III) and Cr(VI). Trivalent chromium is an essential trace element which is necessary for the formation of glucose tolerance factor and the metabolism of insulin. Hexavalent chromium is a strong oxidizing agent.

3.2 Application of chromium

Chromium is regarded with great interest because of its high corrosion resistance and hardness. A major development is the discovery that steel could be made highly resistant to corrosion and discoloration by adding chromium to form stainless steel. This application, along with chrome plating (electroplating with chromium) are currently the highest-volume uses of the metal. Chromium and ferrochromium are produced from the single commercially viable ore, chromite, by silicothermic or aluminothermic reaction or by roasting and leaching processes.

3.3 Sources

Chromium is obtained from chromite ores ($FeOCr_2O_3$). Combustion and the processing of ore discharge primarily Cr(III) into the environment as chromium oxide; however, a small amount of Cr(VI) does appear in fly-ash of coal fired power plants and from chromate manufacturing sites. Most released chromium in the environment results from various sources of human activities. The primary users of chromium compounds are chemical, metallurgical and refractory industries.

Commercial applications include stainless and alloy steels, electroplating, catalyst, corrosion inhibition, pigments, refractory products, glassware-cleaning solutions, wood preservatives and tanning agents for leather. In addition, trivalent chromium salts, including chromium chloride, niacin-bound chromium (III) or chromium polynicotinate and chromium picolinate, are used as micronutrients and dietary supplements.

3.4 Toxicity of chromium

Acute toxicity**;** Acute poisoning likely occurs through the oral route. Ingestion of hexavalent chromium may cause both local and systemic involvement, which include intense gastrointestinal irritation or ulceration and corrosion, epigastric pain, nausea, vomiting, diarrhea, vertigo, fever, muscle cramps, hemorrhagic diathesis, toxic nephritis, renal failure, intravascular hemolysis, circulatory collapse, peripheral vascular collapse, liver damage, acute multi-system shock, coma, and even death. The severity of the involvement depends on the dose. In addition, acute chromic acid exposure produces local inflammation, ulceration of the skin and hypersensitivity dermatitis, while in severe cases, systemic toxicity can be occurred. Inhalation exposure in occupational workers with chromate spray paint, zinc chromate primer paint, chromic acid vapor and Cr(VI) fumes can cause bronchial asthma, pulmonary edema, pneumoconiosis, and metal fume fever.

The International Agency for Research on Cancer (IARC) and the US Toxicology Program recognize hexavalent chromium known as a human carcinogen. The increased risk of lung cancer is associated with the inhalation of Cr(VI) in the occupational setting, primarily in population of workers refining chromite ore or producing chromate pigments. The risk of lung cancer following exposure to Cr(VI) increases with the duration of exposure; the mean latency period ranges from 13 to 30 years.

Table 3 The physical of chromium.

Properties	
General properties	
Name	Chromium
symbol	Cr
number	24
Element category	transition metal
Standard atomic weight	51.9961
Electron configuration	[Ar] $4s^1 3d^5$
Electrons per shell	2, 8, 13, 1
Physical properties	
Phase	solid
Density (near r.t.)	7.19 $g \cdot cm^{-3}$
Liquid density at m.p.	6.3 $g \cdot cm^{-3}$
Melting point	2180 K, 1907 °C, 3465 °F
Boiling point	2944 K, 2671 °C, 4840 °F
Heat of fusion	21.0 $kJ \cdot mol^{-1}$
Heat of vaporization	339.5 $kJ \cdot mol^{-1}$
Molar heat capacity	23.35 $J \cdot mol^{-1} \cdot K^{-1}$
Atomic properties	
Oxidation states	**6**, 5, 4, **3**, 2, 1, -1, -2
Electronegativity	1.66 (Pauling scale)
Ionization energies	1st: 652.9 $kJ \cdot mol^{-1}$
(more)	2nd: 1590.6 $kJ \cdot mol^{-1}$
	3rd: 2987 $kJ \cdot mol^{-1}$
Atomic radius	128pm
Covalent radius	139±5 pm

Source: Wikipedia (2012)

4. Phenol

4.1 Characteristics of phenol

Phenol is also known as carbolic acid, a white crystalline solid with a sweet tarry odor, commonly referred to as a “hospital smell”. Its chemical formula is C_6H_5OH and chemical name is hydroxybenzene. The structure of phenol consists of a hydroxyl group (-OH) bonded to a phenyl ring. Thus, it is an aromatic compound which slightly acidic. The structure of phenol is shown in Figure 16. The phenol molecule has weak tendencies to lose the H^+ ion from the hydroxyl group, resulting in the highly water-soluble phenolate anion ($C_6H_5O^-$), and also called phenoxide anion. Compared to aliphatic alcohols, phenol shows much higher acidity. It even reacts with aqueous NaOH to lose H^+, whereas aliphatic alcohols do not. Anywhere, many carboxylic acids are more acidic than phenol. One explanation for the increased acidity over alcohols is the resonance stabilization of the phenoxide anion by aromatic ring. The negative charge on oxygen is shared by the ortho and paracarbon atoms. In another explanation, increased acidity is the result of orbital overlap between the oxygen's lone pairs and the aromatic system. In a third, the dominant effect is the induction from the sp^2 hybridized carbons which is more powerful inductive withdrawal of electron density that is provided by the sp^2 system compared to a sp^3 system, allows for great stabilization of the oxyanion. The properties of phenol are shown in table .4

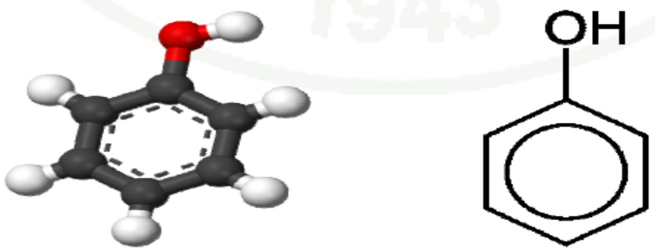

Figure 16 The structure of phenol.

Source: Wikipedia (2012)

4.2 Applications of phenol

Phenol is used in the production of drugs (it is the starting material in the industrial production of aspirin), herbicides, and synthetic resins (Bakelite, one of the first synthetic resins to be manufactured, is a polymer of phenol with formaldehyde). Phenol is the preferred chemical in use of embalming bodies for anatomical use and study because of its ability to preserve tissues for extended periods of time. Phenol is also used in the preparation of cosmetics including sunscreens, hair dyes, and skin lightening preparations. Compounds containing phenol moieties can be used to prevent ultraviolet light which induced hair and skin to be damaged, due to the UV absorbing properties of the aromatic ring of the phenol.

4.3 Toxicity of phenol

Inhalation and dermal exposure to phenol is highly irritating to the skin, eyes, and mucous membranes in humans. Phenol is considered to be very toxic to humans through oral exposure, with ingestion of 1 g reported to be lethal, with symptoms including muscle weakness and tremors, loss of coordination, paralysis, convulsions, coma, and respiratory arrest. Blood changes, liver and kidney damage, and cardiac toxicity including weak pulse, cardiac depression, and reduced blood pressure have been reported in humans acutely exposed to phenol by the oral route. Acute (short-term) animal tests, such as the LD50 tests in rats, mice, and rabbits have shown phenol to have high acute toxicity from oral exposure. Long-term inhalation exposure to phenol in animal studies has shown effects on the liver, kidney, respiratory, cardiovascular, and central nervous systems.

Table 4 The properties of phenol.

General properties	
Molecular formula	C_6H_5OH
Molar mass (g/mol)	94.11
Apprearance	white crystalline solid
Physical and chemical properties	
Density (g/cm³)	1.07
Melting point (°C)	40.5
Boiling point (°C)	181.7
Solubility in water (g/100 ml)	8.3 (20 °C)
Acidity (pKa)	9.95

Source: Wikipedia (2012)

OBJECTIVES

There are three main objectives for this work.

1. To prepare and characterize the bamboo charcoal which will be activated by nitric acid.

2. To study the adsorption capacity of Cr(III) and phenol onto activated bamboo charcoal compared to bamboo charcoal.

3. To study on the adsorption isotherm of phenol on the activated bamboo charcoal.

LITERATURE REVIEWS

They have been many researches study on the adsorption of metal ions and phenol on activation charcoal surface. Reviews of some researches were summarized in this part.

El-Hendawy *et al.*(2001) studied the three types of adsorbing carbons which were obtained from an agricultural byproduct, Dried, crushed, corncobs were carbonized at 500°C and steam activated, or activated with H_3PO_4. The products were characterized by N_2 adsorption at 77 K, using the BET method. Adsorption capacity was demonstrated by the iodine and phenol numbers, and the isotherms of methylene blue and Pb(II) ions, from aqueous solutions. A char by carbonization at 500°C which yields a poorly developed wide-pored carbon with high capacity for iodine and Pb(II)ions. It was ascribed to the presence of an incompletely carbonized residue with unsaturated bonds and oxygen complexes. Steam-activated carbons were developed porosity with that temperature, essentially microporous. Thermal activation under the single-step steam pyrolysis route, at 700°C, provided better adsorbing carbon with much developed porosity and enhanced carbon product. Chemical activation by H_3PO_4 at 500°C proved very effectively in producing high quality activated carbon with well-developed porosity and high adsorption capacity for both organic and inorganic substrates. Removal of Pb(II) ions from an unbuffered solution took place on specific adsorption sites.

Dahbi *et al.* (2002) studied the ability of bone charcoal to remove Cr(III) from aqueous solutions. The adsorbent was first characterized and then the adsorption was studied as a function of time and amount of charcoal. Tests were carried out with synthetic solutions by using Cr(III) concentrations (500 mg/L) which were similar to those found in some effluents of Moroccan tannery industries. Higher 90% Cr(III) removal efficiencies were obtained at pH 3.5 using 3 g. of bone charcoal and a stirring time for 30 min. The results of Cr(III) removal by all sieved fractions of bone charcoal had shown the same interesting capabilities for Cr(III) retention. The studied of pretreatment of bone charcoal by nitric acid led to an increase its specific surface area but it induced a drastic reduction in Cr(III) elimination abilities. Adsorption tests were also carried out using calcinated bone charcoal. Their results showed a similar percentage of Cr(III) retention to found with untreated bone charcoal. And the double treatment of bone charcoal with HCl and NaOH provided an enhancement of Cr(III) retention.

Rivera and Sanchez (2003) studied the adsorption of Cr(III) in aqueous solution on a series of ozonised activated carbons in term of the effect of oxygenated surface groups on the adsorption process. Their studied was carried out to determine the adsorption isotherms and the influence of the pH on the adsorption of metal. The adsorption capacity and affinity of the adsorbent for Cr(III) increased because of the increase in oxygenated acid groups on the surface of the activated carbon. That was implied that electrostatic-type interactions predominate in the adsorption process and the adsorption of Cr(III) on the original carbon indicated that other forces also participate in the adsorption process. The ionic exchange of protons in the $–C\pi–H_3O^+$ interaction for Cr(III) accounts for the adsorption of cationic species in basic carbons with positive charge density. The studied of the influence of pH on the adsorption of Cr(III) was showed that, the maximum adsorption occurred when the charge of the carbon surface was opposite that of the species of Cr(III) present at the pH of the experiment. Their results confirmed that electrostatic interactions predominate in the adsorption process.

Terzyk (2003) studied four carbons with different chemical compositions of the surface layer but almost identical porosity. In the first part, he studied the method of carbon porosity characterization (ND method) which was implied that the porosity had been changed much after the chemical modification of carbons. It was showed that the ND method leads to the same results as the DFT (density functional theory) did. In the next part, the TPD results for D43/1 carbons (initial, modified with HNO_3, fuming H_2SO_4, and with NH_3) were described. The thermogravimetric analysis of phenol adsorption shows that the amount of chemically bonded molecules was small. Then it was showed that the adsorption at the acidic pH (1.5) level was lower for all studied carbons than that at the neutral one. The description of the isotherms applying adsorbability, quasi-Freundlich and DA models, together with enthalpy measurements, lead to the mechanism of phenol adsorption at both pH values. The mechanism was confirmed by some empirical correlations. The analysis of the average hysteresis on adsorption–desorption isotherms as well as the comparison of phenol adsorption in oxic and anoxic conditions leads to the mechanism of irreversible phenol adsorption. It was suggested that the irreversibility was caused by two effects: the creation of strong complexes between phenol and surface carbonyl and lactones as well as by the polymerization.

Babel and Kurniawan (2004)**,** in their study, the technical feasibility of coconut shell charcoal (CSC) and commercial activated carbon (CAC) for Cr(VI) removal was investigated in batch studies using synthetic electroplating wastewater. Both granular adsorbents were made of coconut shell (Cocosnucifera L.), an agricultural waste from local coconut industries. Surface modifications of CSC and CAC with chitosan and/or oxidizing agents, such as sulfuric acid and nitric acid, respectively, were also conducted to improve removal performance. The results of their Cr(VI) removal performances were statistically compared. CSC and CAC, which had been oxidized with nitric acid had higher Cr(VI) adsorption capacities (CSC: 10.88, CAC: 15.47 mg/g) than oxidized with sulfuric acid (CSC:4.05, CAC: 8.94 mg/g) and non-treated CSC coated with chitosan (CSCCC: 3.65 mg/g), respectively. The surface modification of a carbon adsorbent with a strong oxidizing agent generated more adsorption sites on their solid surface for metal adsorption.

Özkaya (2006), the potential of activated carbon for phenol adsorption from aqueous solution was studied. Batch kinetics and isotherm studies were carried out to evaluate the effect of contact time, initial concentration, and desorption characteristics of activated carbon. The equilibrium data in aqueous solutions was represented by the isotherm models. Desorption studies to recover the adsorbed phenol from activated carbon performed with NaOH solution. The pore diffusion and first-order kinetic models were compared. The diffusivity rate (D/r^2) and first-order desorption rate (k_D) constants were determined as 6.77×10^{-4} and 3.924×10^{-4} s^{-1}, respectively. The low value of desorption kinetic constant indicates that the adsorbed phenol remains almost stable on the adsorbent and can be recovered from the adsorbent by desorption with sodium hydroxide. The results showed that the first-order kinetic model represented the data for NaOH desorption more suitable fitting than the pore diffusion model. The results also demonstrated that the Langmiur model fitted the experimental data a little better than the three parameter models, Redlich–Peterson and Toth.

Mohan *et al.* (2006) studied a low cost activated carbon (ATFAC) which was prepared from coconut shell fibers, then characterized and utilized for Cr(III) removal from water/wastewater. A commercial activated carbon fabric cloth (ACF) was also studied for comparative evaluation. All the equilibrium and kinetic studies were conducted at different temperatures, particle size and pH. The Langmuir and Freundlich isotherm models were applied. The Langmuir model best fit the equilibrium isotherm data. The maximum adsorption capacities of ATFAC and ACF at 25 ˚C were 12.2 and 39.56 mg/g, respectively. The Cr(III) adsorption increased with an increase in temperature (10 ˚C: ATFAC-10.97 mg/g, ACF—36.05 mg/g; 40 ˚C: ATFAC-16.10 mg/g, ACF-40.29 mg/g). The adsorption of Cr(III) follows the pseudo-second-order rate kinetics. From kinetic studies, various rate and thermodynamic parameters such as effective diffusion coefficient, activation energy and entropy of activation were evaluated. The sorption capacity of activated carbon (ATFAC) and activated carbon fabric cloth was comparable to many other adsorbents/carbons/biosorbents utilized for the removal of trivalent chromium from water/wastewater.

Mohamed *et al.* (2006)**,** in their work, sawdust was used as a source material to prepared activated carbons by chemical activation with sulphuric acid. Texture properties of carbons were determined by measuring the adsorption of nitrogen at 77 K and of carbon dioxide at 298 K. The nitrogen adsorption isotherms were interpreted by BET equation and αs-method while carbon dioxide adsorption results were interpreted by applying the D–R equation. The nature of carbon surface functionalities was studied by FT-IR spectroscopy and Boehm titration method. The adsorption of phenol, hydroquinone, resorcinol and catechol from aqueous solution at 298 K on to these carbons had been investigated. FT-IR showed an acidic character with carboxylic groups were essentially fixed along with lactonic and phenolic groups. The equilibrium data fit the Langmuir isotherm well. The amounts of phenols adsorbed, without exception decreased, with increasing the concentration of acid groups on the carbon surface. For each carbon, the amount of phenol adsorbed follows the order phenol > hydroquinone > resorcinol > catechol.

Phan *et al.*(2006) studied the different fibrous activated carbons which were prepared from natural precursors (jute and coconut fibers). Physical activation consisted of the thermal treatment of raw fibers at 950 °C. In chemical activation, the raw fibers were impregnated in a solution of phosphoric acid and heated at 900 °C in an inert atmosphere. The adsorption properties of the activated carbons were tested towards pollutants representative of industrial effluents: phenol, the dye Acid Red 27 and Cu(II) ions. Their method led to an interesting porosity (S_{BET} up to 1500 m^2/g), which enabled a high adsorption capacity for micropollutants like phenol (reaching 181 mg/g).

Polat *et al.* (2006) studied a raw lignitic coal from Soma which was determined its potential as an adsorbent for phenol removal from wastewaters. Kinetic batch tests demonstrated that phenol could be completely removed from solution given sufficient solids loading and reaction time. The adsorption capacity of 10 mg/g obtained with the lignite was low compared to those achievable with activated carbons (around 300 mg/g). When normalized for the surface area, the adsorption capacity was much larger for the lignite (1.3 mg/m^2) than that observed with activated carbons (0.05–0.3 mg/m^2). Hydrogen-bonding of the phenolic –OH with the oxygen sites on the lignite surface was the most likely mechanism for adsorption. Though water molecules also have affinity for the same oxygen sites, lateral benzene ring interactions make phenol adsorption more favorable. Since phenol molecules adsorbed in this fashion would project their benzene rings into solution, formation of a second layer through the action of the dispersive π–π interactions between the benzene rings was very likely. Residual water quality with respect to major elements and heavy metals was within acceptable limits defined by the ASTM standards. Dissolution of organic matter from the lignite was also observed to be negligible.

Kumar *et al.* (2007) studied the adsorption behavior of phenol and 4-nitrophenol on granular activated carbon from a basal salt medium (BSM) at pH ≈7.1 and temperature ≈30 ˚C. The units for measurements reported in these models were found to be diversed. Six models of Freundlich, Langmuir, Redlich–Peterson, Radke–Prausnitz, Toth and Fritz Schlunder had been fitted to the data of phenol/activated carbon and 4-nitrophenol/activated carbon systems of the present studies using nonlinear regression technique. 4-Nitrophenol was found to be more adsorbed than phenol. The kinetics of the adsorption were found to be intra-particle diffusion controlled with diffusion coefficient values of the order of 10−13 m^2/s. Three distinct phases of kinetics – rapid, medium, and slow – have been observed in his study.

Natale *et al.* (2007) studied the adsorption isotherms of chromium ions in aqueous solution which had been experimentally measured on a granular activated carbon (GAC) and on a char of South African coal (CSAC). The results showed that the adsorption capacity for the GAC strongly depended on solution pH and salinity, with maximum values around 7 mg/g at neutral pH and low salinity levels. The CSAC showed a smaller adsorption capacity, near 0.3 mg/g, which was slightly decreased by increasing pH and salinity levels. Chromium adsorption mainly depended on the availability of chromium ions in solution and on the occurrence of redox reactions between the surface groups and the Cr(VI) which lead to the formation of Cr(III). The reduction of Cr(VI) and the following sorption of Cr(III) cations were appeared as the leading mechanism for chromium uptake on the CSAC. A similar behavior could be observed for the GAC at pH below 3. On the contrary, at pH > 7, the multicomponent competitive adsorption of Cr(VI), OH^- and Cl^- had been considered.

Hameed *et al.* (2007) studied the preparation of bamboo activated carbon by physiochemical activation with potassium hydroxide (KOH) and carbon dioxide (CO_2) as the activating agents at 850 ˚C for 2 h. The adsorption equilibrium and kinetics of methylene blue dye on such carbon were then examined at 30 °C. Adsorption isotherm of the methylene blue (MB) on the activated carbon was determined and correlated with isotherm equations. The equilibrium data for methylene blue adsorption well fitted to the Langmuir equation, with maximum monolayer adsorption capacity of 454.2 mg/g. The two simplified kinetic models including pseudo-first-order and pseudo-second-order equation were selected to follow the adsorption processes. The adsorption of methylene blue could be best described by the pseudo-second-order equation.

Stavropoulos *et al.* (2007) examined the modified activated carbons with tailored adsorption capacity properties. The modification of an activated carbon was performed using partial oxygen gasification, nitric acid treatment, urea impregnation followed by pyrolysis and pyrolysis in a urea saturated stream. The surface properties of the produced samples were estimated by the multi basic titration method of Boehm and by the CO/CO_2 gas evolution profiles, while pore structure development was measured by the N_2 and CO_2 gas adsorption isotherms. Oxygen gasification resulted in samples with surface area was slightly lower than the raw activated carbon; the introduction of surface functional groups depended upon the severity of the treatment: carbonylic and phenolic type groups were introduced in all partially gasified samples, while low temperatures and short reaction times enhanced the basic character of the carbon. The presence of surface functional groups affected the adsorption capacity of the produced samples for the removal of specific pollutants such as phenols. Urea treated samples with a basic character and high nitrogen content presented the highest phenol uptake capacity; nitric acid treated carbons and oxygen gasified samples presented an acidic surface functionality and a low phenol adsorption capacity. The beneficial role of nitrogen on phenol adsorption was attributed to adsorbate–adsorbent interactions.

Podkos and Nieszporek (2007) studied the surface heterogeneity of activated carbons which was prepared from polyacrylonitrile (PAN) and polyethylene terephthalate (PET) were usually characterized by adsorption energy distribution (AED) functions and could be estimated from the experimental adsorption isotherms by inverting integral equation. All experimental data of phenol adsorption from aqueous solution on activated carbon have been taken from literature. The adsorption energy distribution functions for phenol adsorption, generated by application of regularization method have been verified. The Grand Canonical Monte Carlo (GCMC) simulation technique has been used as verification tool. The definitive stage of verification was comparison of experimental adsorption data and those obtained by utilization GCMC simulations. Necessary information for performing of simulations has been provided by parameters of AED functions calculated by regularization method. From the verification method, the GCMC simulation technique has been used based on square lattice with a Dubinin–Astakhov distribution of adsorption energy. The final stage of verification was comparison of experimental data and obtained by use of GCMC simulations. The agreement of the experimental isotherms data with predictions of simulations was satisfactory. It could be confirmed that the reliability of AED functions obtained based on regularization method (INTEG algorithm) and it independently confirms the usefulness of their method for studying heterogeneity of solid adsorbents.

Chan *et al.* (2008) studied activated carbons which were produced by thermal activation of bamboo with phosphoric acid and used for adsorption of acid dyes. Two acid dyes with different molecular sizes were used, namely Acid Yellow 117 (AY117) and Acid Blue 25 (AB25). They found that dye with smaller molecular size, AB 25, was readily adsorbed onto the carbon while the larger size dye, AY117, showed low adsorption.

Ip *et al.* (2008) studied high surface area activated carbons that have been produced from the natural biomaterial bamboo, using phosphoric acid. Three of bamboo derived active carbons, surface areas 1337, 1628 and 2123 m^2/g were assessed for their ability to adsorb Acid Red 18 dye from aqueous solution and compared with three conventional adsorbents (activated carbon F400, bone char and peat). They found that Langmuir–Freundlich equation provided the best overall correlation of data and adsorption capacities of two of the selected bamboo derived carbons were much greater than the capacities of the other three adsorbents.

Wang *et al.* (2008) studied the activated carbon with high specific surface area and considerable mesopores which were prepared from bamboo scraps by phosphoric acid activation. Under the conditions of impregnating bamboo with 80% H_3PO_4 at 80^0C for 9 days and activation at 500^0C for 4 h, the prepared activated carbon had the highest mesopore volume of 0.67 cm^3/g, a specific surface area of 1567 m^2/g, and the mesopore ratio reached 47.18%. The considerable difference in the adsorption capacity between CO_2 and the other gases was observed, which would be interested for the adsorptive separation/purification of gaseous CO_2 from its mixtures, especially from mixtures with N_2 and/or O_2.

Shen *et al.* (2008) studied the review of the modification of porous carbon with various methods, such as, acid treatment, oxidization, ammonization, plasma, microwave treatment. Modification of porous carbon via acidic, thermal treatment were not by far, the most studied technique, might be attributed to its simplicity, availability of oxidization process. Generally, oxidization treatment of porous carbon was favorable for enhancing its adsorption for polar molecules while thermal treatment was desired for adsorption for non-polar molecules. The nitrogen functional groups could improve its adsorption for odor gases and acidic molecules. These methods could change the pore structure of porous carbon in little or large degree. In their studied, the modification methods were illustrated and compared, some new methods were also reviewed. The functional groups on surface were determined by the treatment methods, the amminization could increase its basic property while the oxidization commonly improved its acids.

Aber *et al.* (2009) studied the preparation of activated carbon fiber (ACF) from Kenaf natural fibers using K_2HPO_4. Optimized conditions were: carbonization at 300 °C, impregnation with 30% w/v K_2HPO_4 solution and activation at 700 °C for 2 h with the rate of achieving the activation temperature equal to 2 °C min^{-1}. The equilibrium data of phenol and p-nitrophenol adsorption on the prepared ACF were fitted to the Langmuir isotherm. The maximum adsorption capacities of phenol and p-nitrophenol on the prepared ACF are 140.84 and 136.99 mg/g, respectively. The adsorption process followed the pseudo-first-order kinetic model.

Ahmad and Hmeed (2009) studied the adsorption potential of bamboo waste based granular activated carbon (BGAC) to remove C.I. Reactive Black (RB5) from aqueous solution using fixed-bed adsorption column. The effects of inlet RB5 concentration (50–200 mg/L), feed flow rate (10–30 mL/min) and activated carbon bed height (40–80 mm) on the breakthrough. The highest bed capacity of 39.02 mg/g was obtained using 100 mg/L inlet dye concentration, 80 mm bed height and 10 mL/min flow rate. The results of adsorption data were fitted well to the Thomas and Yoon–Nelson models with coefficients of correlation $R^2 \geq 0.93$ at different conditions. The BGAC was shown to be suitable adsorbent for adsorption of RB5 using fixed-bed adsorption column.

Guolin *et al.* (2006) studied the adsorption processes of Cr(VI) from aqueous solution onto a granular activated carbon (GAC) and a modified activated carbon (MAC) with nitric acid. The surface characteristics showed that the MAC had a lower surface area, lower pH_{IEP} and more oxygen functional groups compared with the GAC. Experimental equilibrium data were showed the Langmuir isotherm model fit better than the Freundlich isotherm for both MAC and GAC and the MAC had a higher Cr(VI) adsorption capability, with 16.1mg/g, compared with GAC, which had a capacity of 6.40 mg/g. The breakthrough curve for the adsorption column tested was obtained in a continuous adsorption bed experiment, and it would need, under continuous adsorption conditions, a minimum amount of 4.39 g/l for MAC, whereas under batch conditions, 2 g/l was enough for MAC to achieve the same removal of Cr(VI) with an initial concentration of 25 mg/l.

Ip *et al.* (2009) studied the adsorption of a large reactive dye, Reactive Black 5 dye, onto two bamboo activated carbon using phosphoric acid in a two stage activation process and three adsorbents, carbon F400, bone char and peat, were studied. The monolayer saturation adsorption capacities for Reactive Black 5 were determined by the Langmuir isotherm analysis and were: 176, 157, 7, 447 and 545 mg dye/g adsorbent for active carbon F400, bone char, peat, bamboo carbon (2123 m^2/g) and bamboo carbon (1400 m^2/g), respectively. The Redlich–Peterson was the best fit experimental equilibrium correlation. The effect of adding salt, in the form of sodium phosphate, on the adsorption capacities was found to increase the adsorption capacities of both bamboo carbons to over 900 mg/g.

Chan *et al.* (2009) prepared activated carbon by using phosphoric acid treat with waste bamboo scaffolding and activated at 400 or 600 °C and studied acid to bamboo ratio (Xp) up to 2.4. The BET surface area was increased with increasing Xp and activating temperature. The produced carbons were tested for its dye adsorption capacities and used two acid dyes with different molecular sizes, namely Acid Yellow 117 (AY117) and Acid Blue 25 (AB25). In a single component system, it was found that dye with smaller molecular size, AB25, was readily adsorbed onto the carbon while the larger size dye, AY117, showed little adsorption. A binary AY117–AB25 mixture was used to test the possibility of the molecular sieve effect. Furthermore, experimental results were fitted to equilibrium isotherm models, Langmuir, Freundlich and Sips for the single component system.

Ghosh (2009) studied two materials, fresh activated carbon (AC) and waste activated carbon (WAC) which were pretreated by heating with sulfuric acid and nitric acid at high temperature to prepare several grades of adsorbents to evaluate their performance on Cr(VI) removal from aqueous phase. Effects of temperature, agitation speed and pH were tested, and optimum conditions were evaluated. Kinetic study was performed under optimum conditions with several grades of modified adsorbents to know the rates of adsorption. Batch adsorption equilibrium data followed both, Freuindlich and Langmuir isotherms. Maximum adsorption capacity ($q_{\max}$) of the selected adsorbents was treated with sulfuric acid (MWAC 1) and nitric acid (MWAC 2), calculated from Langmuir isotherm were 7.485 and 10.929 mg/g, respectively.

Chand *et al.* (2009) studied effects of oxidation using HNO_3 on the properties of the carbonized wheat and barley straw and studied the different properties such as specific surface area, PZC, total surface acidic groups as well as FT-IR and TG–DTA. From the experimental data showed that a small decreased in the specific surface area due to pore blockage was observed after oxidation. After oxidation, the acidity was increased and the point of zero charge shifted from approximately pH 9 to pH 2 in both types of carbon. By the oxidation with nitric acid, carboxylic groups were produced as shown by absorption peaks at 1750 cm^{-1} in the FT-IR spectra. Boehm titration results showed that the number of carboxyl groups increased by approximately 11-fold after oxidation. The oxidized carbon samples were compared with the original carbon samples for Cr(III) adsorption. The observed oxidized carbons exhibit high adsorption efficiencies for Cr(III) ions compared to the original carbonized straws and can be correlated to the decrease in PZC which is mainly due to the increasing in carboxylic functional groups in the oxidized carbonized straws.

Tangjuank *et al.* (2009) studied the activated carbon produced from cashew nut shells using potassium hydroxide activation at 850 °C in N_2 and CO_2 atmosphere was used as an adsorbent for the removal of chromium ions from aqueous solutions. The adsorption of Cr(III) ions on activated carbon was studied. The effect of experimental parameters such as, pH of initial concentration of Cr(III) solutions, contact time, dosage of adsorbent and initial concentration of Cr(III) solutions was investigated. The adsorption process depends on the optimal conditions on the data from the experiments. These were initial pH 3.5 of Cr(III) solution, contact time 60 min and 1.2 g activated carbon/solution 100 mL at 100 mg/L of initial concentration of Cr(III) solution. The Freundlich and Langmuir isotherm fitted well to data of Cr(III) adsorption. The theoretical for chromium uptake capacity from Langmuir isotherm was 13.93 mg/g
which was very close to the actual value gotten from the actual experimental value (12.91 – 14 mg/g.).

Mui *et al.* (2010) studied a series of activated carbons which were prepared from bamboo by activation with HCl, HNO_3 and H_2SO_4 and studied in term of operating variables such as activation temperature, impregnation ratio and holding time. The resultant carbons were evaluated for the yield, surface area, pore size distribution, pH, elemental composition and ash. At an impregnation ratio (the mass ratio between bamboo/acid) of 1, activated carbon with BET surface area and micropore volume as high as 553 m^2/g and 0.239 cc/g was obtained at 1173 K using

H_2SO_4 as an activating agent. The amount of nitrogen adsorbed by activated carbons from acid-impregnated bamboo were : $H_2SO_4 > HCl > HNO_3$.

MATERIALS AND METHODS

Materials

1. Apparatus

1.1 Atomic absorption spectrophotometer (AAs : Perkin Elmer, AA analyst800)

1.2 UV-Vis spectrophotometer (Perkin Elmer, Lambda 35)

1.3 Fourier transform infrared spectrometer (FT-IR : Perkin Elmer, System2000)

1.4 Scanning electron microscope (SEM : Philips, XL30)

1.5 Microbalance (Mattler Toledo, AL 204)

1.6 Rotary shaker (Clifton, NE5-2BD CE)

1.7 pH meter (Inolab level 1, 8F93)

1.8 Oven (Precision,16EG)

1.9 Sieve mesh 150 µm

2. Reagents

2.1 Phosphoric acid (H_3PO_4, AR. grade, Ajax Finechem, Aukland, New Zealand)

2.2 Nitric acid (HNO_3, AR. Grade, Lab-scan, Bangkok, Thailand)

2.3 Phenol (C_6H_6O, AR. grade, Carlo Erba, Rodano, Milan, Italy)

2.4 Chromium standard for atomic absorption 1000 mg/l ($CrCl_3.6H_2O$, AA. Grade, Carlo Erba, Rodano, Milan, Italy)

2.5 Sodium acetate (CH_3COONa, AR. grade, Merck, Darmstadt, Germany)

2.6 Sodium carbonate (Na_2CO_3, AR. grade, Merck, Darmstadt, Germany)

2.7 Sodium thiosulfate ($Na_2S_2O_3.5H_2O$, AR. grade, Merck, Darmstadt, Germany)

2.8 Potassium bromate ($KBrO_3$, AR. grade, BDH, Poole, United Kingdom)

2.9 Potassium bromide (KBr, AR. grade, Merck, Darmstadt, Germany)

2.10 Potassium iodate (KIO_3, AR. grade, Univar, United State of America)

2.11 Potassium iodide (KI, AR. grade, VWR International, England)

2.12 Potassium dihydrogen phosphate (KH_2PO_4, Lab. Grade, Fischer scientific, USA)

2.13 Hydrochloric acid (HCl, AR. grade, Carlo Erba, Rodano, Milan, Italy)

2.14 Starch ($(C_6H_{10}O_5)n$, AR. Grade, Merck, Darmstadt, Germany)

2.15 Acetic acid (CH_3COOH, AR. grade, Merck, Darmstadt, Germany)

2.16 Bamboo charcoal (*Thyrsostachys Siamensis Gamble*)

Methods

1. Preparation of bamboo charcoal

Raw material (bamboo wood, *Thyrsostachys Siamensis Gamble*) was used for preparation of charcoal which was cultivated from Kanchanaburi province, then washed, dried and crushed to size of 1-2 mm and then carbonized at 450 °C by MES 20, (shown in figure 17).

Figure 17 The MES 20 for carbonization.

2. Preparation of activated charcoal

The carbonized charcoal was then ground and sieve to less than 150 µm. After being washed and dried overnight, bamboo charcoal was oxidized with 70% HNO_3 in the ratio between charcoal and HNO_3 equal to 1:3 for 4 hours. The oxidized adsorbent was washed until the pH of rinsing water remained constant. Finally, the samples were dried overnight in an oven and stored in a desiccator. The bamboo activated charcoal (BAC) was used to study the removal efficiency of Cr(III) and phenol studied compared to bamboo charcoal (BC).

3. Surface characterization

3.1 Scanning electron microscope (SEM)

Scanning Electron Microscope Philips XL30 was used to analyze the porosity of bamboo activated charcoal (BAC) compare to bamboo charcoal (BC).

3.2 Fourier transform Infrared Spectrometry (FT-IR)

Bamboo activated carbon (BAC) and bamboo charcoal (BC) samples were studied with Fourier transform Infrared Spectrometry, FT-IR by using KBr technique to obtained functional groups of samples.

4. Cr (III) adsorption studied

4.1 Cr(III) removal efficiency

The change in Cr(III) concentration was determined by using atomic absorption spectrophotometer (AAs) at wavelength 357.9 nm by external standard calibration technique using standard Cr(III) solution 0.5-5.0 mg/L used to be standard calibration curve. Blank solution was set in the same condition as Cr(III) solution in all experiment by using 0.01M acetate buffer. By this method, the minimum detectable concentration is approximately 0.005 mg/L as Cr(III).The example of calculation is also shown in Appendix C.

The Cr(III) removal efficiency (E) of adsorbent on Cr (III) was defined
as equation (7).

$$E(\%) = \left[\frac{C_0 - C_1}{C_0}\right] x100 \qquad (7)$$

Where C_o and C_1 are initial and final concentration of Cr(III) solution (mg/L), respectively.

4.2 Effect of Cr(III) dose

The dependence of Cr(III) sorption on dose was studied in terms of Cr(III) removal efficiency (E) by varying the amount of bamboo activated charcoal (BAC) from 0.01 to 0.25 g. To maximize the Cr removal efficiency, 25 ml 5 mg/L, pH 5 of Cr(III) solution was added to a set of flasks with difference weight of BAC and then placed into the isothermal shaker with agitation speed 200 rpm at 30±1 ^{0}C and contact time 3 hours to reach equilibrium of the solid-solution mixture, the flasks will be then removed from the shaker and the final concentration of Cr(III) in the solution was analyzed by using atomic absorption analysis.

4.3 Effect of pH

To understand the effect of pH, a set of flasks [(50 ml) with fixed dose of BAC and Cr(III) solution (5 mg/L, 25 ml)] with different pH, which was adjusted between pH 3.0 – 6.0 by using acetate buffer, were used to studied. The contents were then shaken in the isothermal shaker with agitation speed 200 rpm at 30±1 ^{0}C for 3 hours. After equilibrium obtained, the flasks were then removed from the shaker and the final concentration of Cr(III) in the solution was analyzed.

5. Phenol adsorption

The change in phenol concentration was determined by UV-VIS spectrophotometric method at wavelength 270.10 nm. by external standard calibration technique using standard phenol solution 2-100 mg/L as standard calibration curve. Blank solution was set in the same condition as phenol solution in all experiment by using 1-strength buffer. The determination of phenol value of activated carbon (American Water Works Association, 1995) which is shown in Appendix A. The example of calculation is also shown in Appendix D.

5.1 Measurement of Moisture

The determination of moisture is carried out by placing a sample of powdered BC and BAC in an uncovered crucible and it is placed in the oven kept at 108±2 ^{o}C along with the lid. Then the sample is cooled to room temperature and weighed again. The loss in weight represents moisture.

5.2 Phenol value

To determine the phenol value, 25 ml of 5 ppm phenol solution at pH 6.5, 0.2 – 0.5 g. of BC, agitation speed 200 rpm and contact time of 30 min were used in the experiment. The residual filtrate after adsorption was determined by UV-VIS spectrophotometric method at wavelength 270.10 nm. The isotherm between % residual phenol and the ratio of the adsorption phenol (X) to amounts of charcoals (M) were plotted in logarithm. The phenol value was determined by the term of X/M at 10% residual phenol of the isotherm as equation (8). The results were compared to BAC.

$$\text{Phenol value} = \frac{90}{\frac{X}{M} at\ 10\%\ residual\ phenol} \times \frac{100 - \%moisture}{100} \qquad (8)$$

5.3 Adsorption equilibrium time

To determine the equilibrium time, 25 ml of 2-20 mg/L phenol solutions at pH 6.5 and 0.2 g of activated charcoal were used. Phenol solutions with initial concentrations were placed in the set of flasks with equal mass of BC, then were kept in isothermal shaker to reach equilibrium. The flasks were then removed from the isothermal shaker in the different time from 30 – 180 minutes and the final concentration of phenol in the solution was analyzed. The equilibrium data of phenol adsorption were fitted to the Langmuir or Freundlich isotherm, and compared to BAC.

6. Statistical analysis

To ensure the precision, repeatability, and reproducibility of the data, all experiments were carried out duplicateiy and the mean values of data sets are presented. In nearly all instances, the accuracy of data was very good, as percentage of the relative standard deviation (or coefficient of variation) was less than 5.0%. The Cr(III) removal efficiency for all types of adsorbents was within the range of ±5.0%. When the relative error exceeded this criterion, the data were disregarded and a third experiment was conducted until the relative error fell within an accept-able range.

Statistical analysis using the paired t -test was used to evaluate the data if there was any significant difference in terms of Cr(III) removal efficiency for two categorical variables between an activated and non-activated bamboo charcoal. This test was conducted if the Kolmogorov–Smirnov test confirmed the normality of the variable distribution ($p > 0: 05$). Otherwise, the Wilcoxon-signed rank test was performed. The analysis of variance (ANOVA) test was used to analyze data, which has three or more than three categorical variables, if the distribution of each variable was normal
($p > 0: 05$). One-way ANOVA test was used to find out if there were any significant differences in terms of Cr(III) removal efficiency due to surface modification between before and after nitric acid treatment in the batch experiments. All statistical tests were performed using Microsoft Excel 2010 with confidence interval of 95%.

RESULTS AND DISCUSSION

1. Characterization of activated charcoal surface

1.1 Scanning electron microscopy (SEM)

Figure 18 shows the scanning electron micrographs of the external structure of two activated charcoal, bamboo charcoal or BC (1a and 2a.) and bamboo activated charcoal or BAC (1b and 2b). From scanning electron micrographs, it can be seen that both of charcoals are full of holes with diameters in the range of 1-5 µm and 1-20 µm, respectively. For BC (1a and 2a) the surface exhibited many thick sheets or layers within the structure. The nitric activation process resulted the cylindrical pores (with large open-ings) which can be seen in the micrographs. The amount of each pores (micropore, mesopore and macropore) is very important to the type of particle being absorbed. The different size molecules will fill different size spaces in the structure.

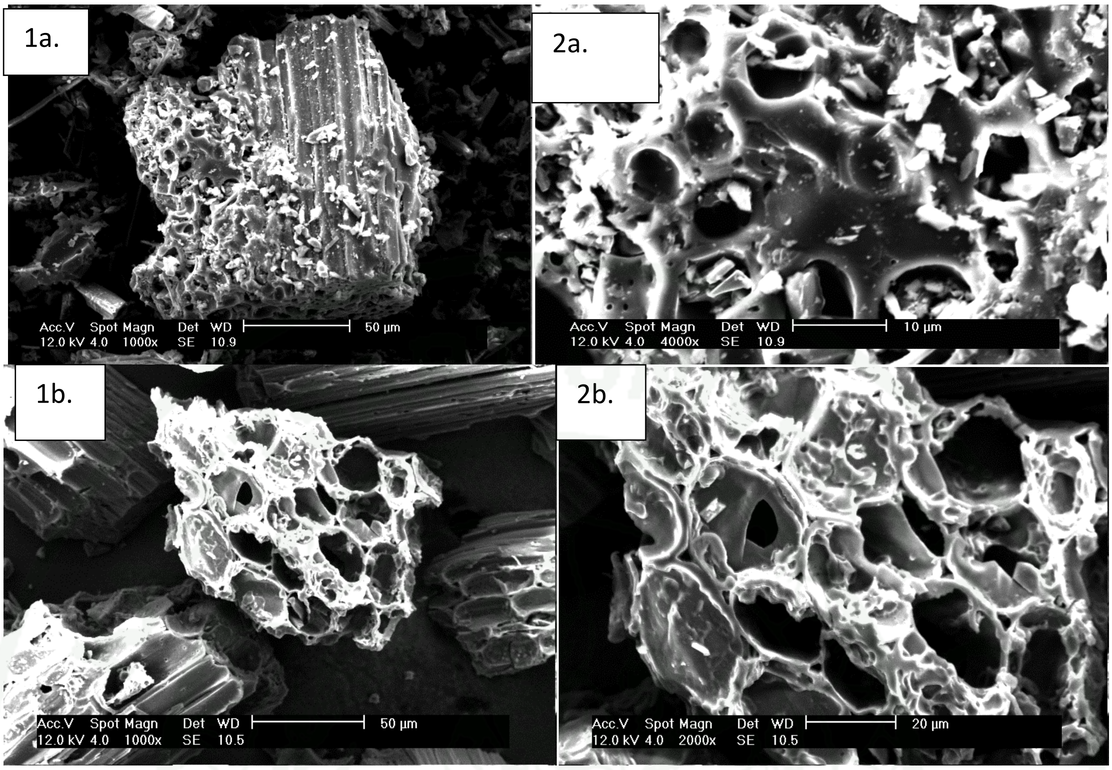

Figure 18 SEM micrographs of (1a.) BC (x1000), (2a.) BC (x4000), (1b.) BAC (x1000), (2b.) BAC (x2000)

1.2 Fourier- transform infrared spectroscopy (FT-IR)

The FT-IR spectrum of BC and BAC are shown in figure 19 and 20. The different in the adsorption of BC and BAC might be associated with the functional group on the its surface which can be enhanced the adsorption. Thus the functional group on the surface of each carbon was studied by FT-IR spectroscopy. The band assignments are shown in table 5.

Table 5 The FT-IR results of bamboo charcoal (BC) and bamboo activated carbon (BAC).

Functional group	Wavelength (cm^{-1})		
	Reference	BC	BAC
Hydroxyl group (O-H Stretching, ROH)	3,450 - 3,350	broad, strong 3,409	broad, strong 3,394
Alkane(C-H Stretching)	2,950 - 2800	(-)	(-)
Ester (ROOR´)	1,750 - 1,650	very weak ~1,700	medium ~1,700
Aromatic (C-C Stretching) Asymmetric and symmetric carboxylate ($(C-O)_2$ Stretching)	1,580 - 1,540	medium 1,583	strong 1,583
Alkane (C-H Bending)	1,350 – 1,470	weak 1,406, 1,358	strong 1,380, 1,354

Table 5 (Continued)

Functional group	Wavelength (cm^{-1})		
	Reference	BC	BAC
Alcoholic (C-O Stretching)	1,200-1,050	weak	weak
Ether (ROR)		1,222, 1,163, 1,107	1,236, 1,089
Cyclic group	880 - 650	weak	very weak
		871, 812, 787	779
Alkane and aromatic (C-C Bending)	500 - 400	weak	very weak
		462, 447	562, 472

Source: Pavia *et al*. (2001)

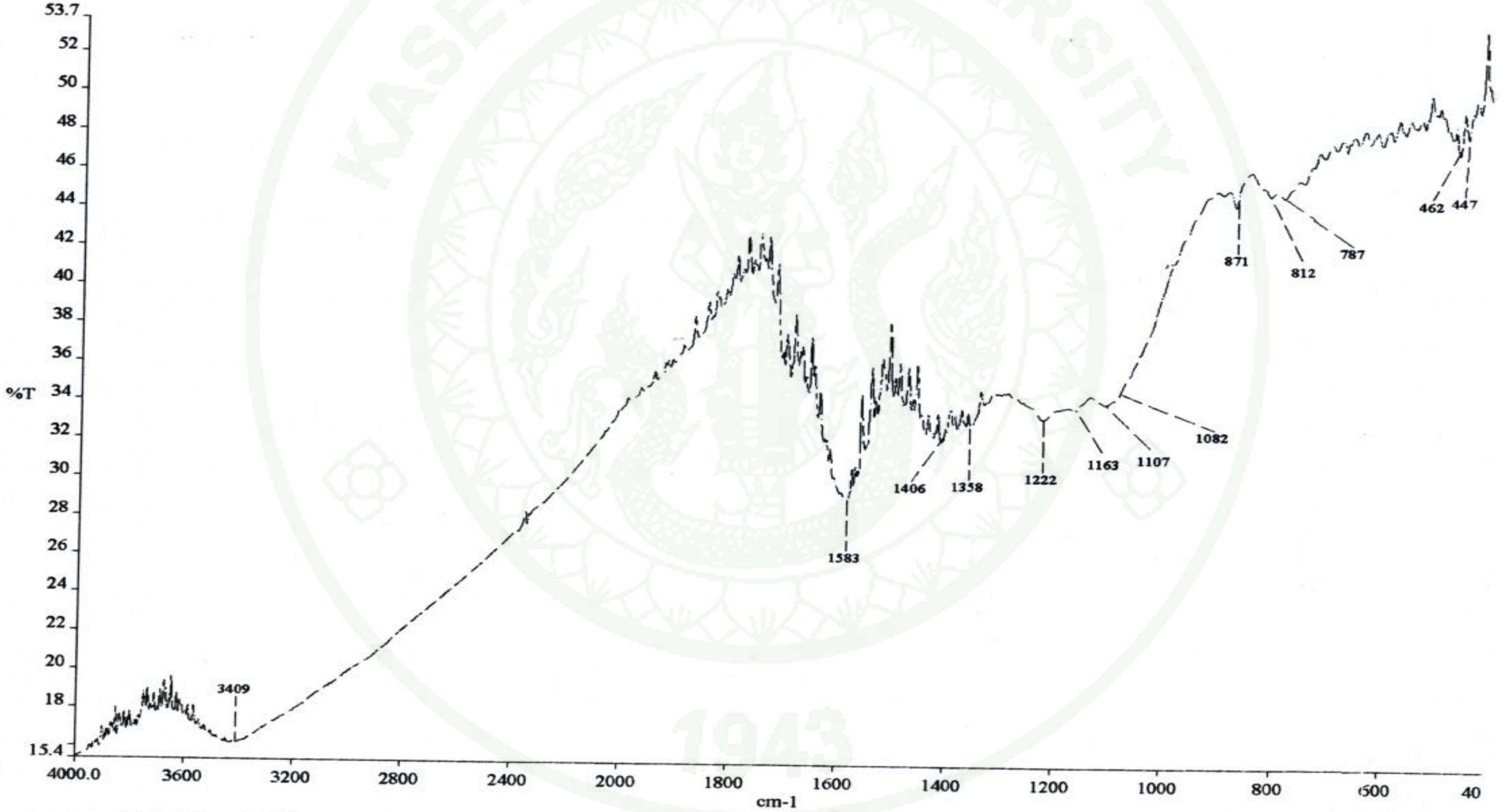

Figure 19 FT-IR spectrum of bamboo charcoal (BC)

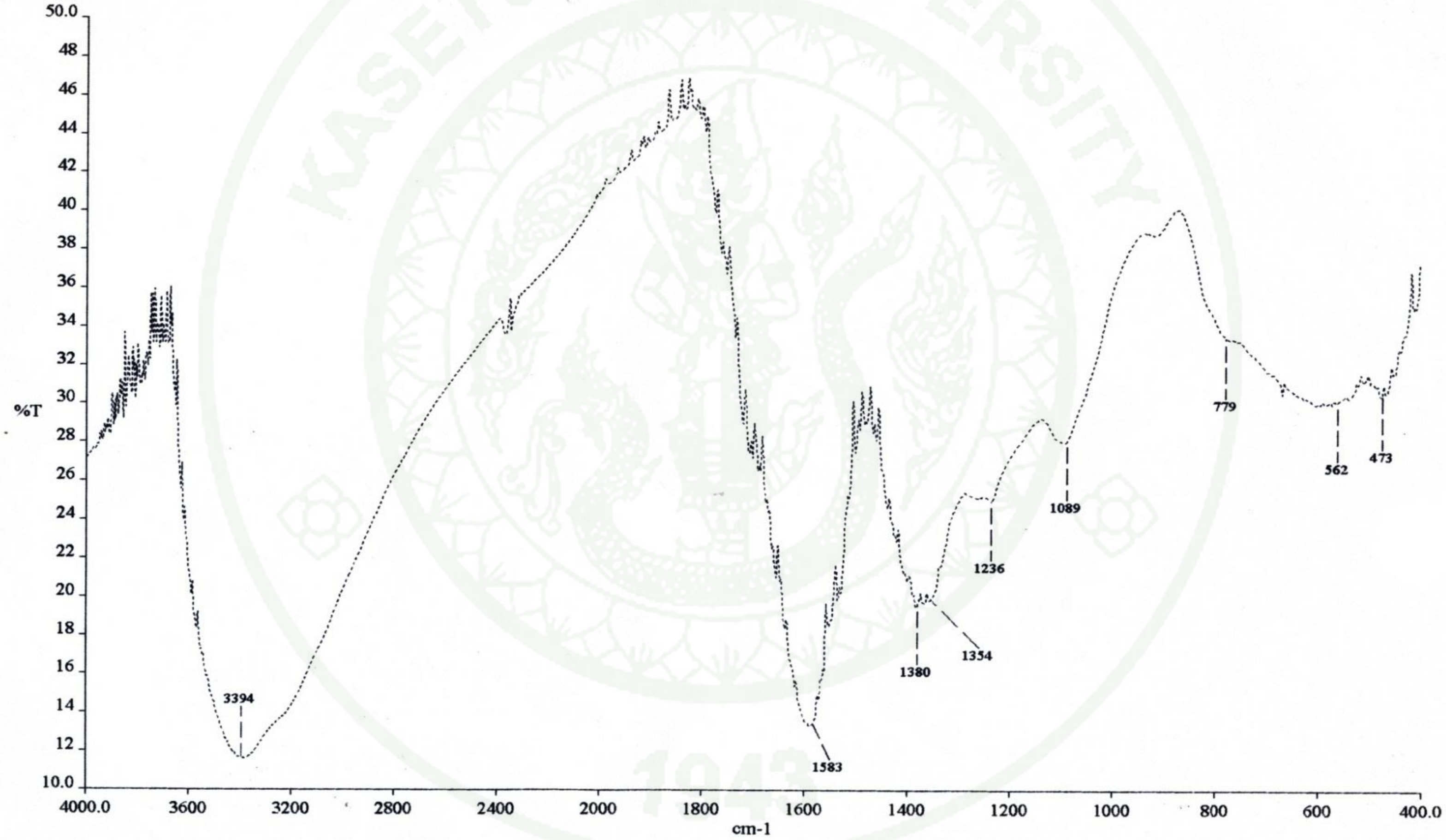

Figure 20 FT-IR of bamboo activated chacoal (BAC)

The FT-IR spectra and their assigned peaks are shown in figure 19, 20 and table 5, respectively. It can be seen that BAC spectrum was similar to BC spectrum. The present of broad peak in the range of 3,450 – 3,350 cm^{-1} was defined as O-H stretching vibration of hydroxyl group. The C-C stretching vibration of aromatic group can be observed in the range of 1,580 – 1,540 $cm^{-1}$and the band at 1,200 - 1,000 cm^{-1} was difficult to assigned because of the overlapping band. The weak absorption band can be observed at 880 – 650 cm^{-1} was attributed to C-H bending of aromatics or cyclic group. From FT-IR spectra, then were shown that BAC and BC had high aromaticity which can cause the negative environment on the surface of BAC that enhanced the positive molecule adsorbed on its surface. Anyway, strong band in 1,800 – 1,540 cm^{-1} region was described to C=O or COO^- group. After the activation by nitric acid, the band in BAC spectrum was stronger than BC spectrum due to the oxidation reaction to change –OH group in to C=O or COO^- group as shown in the equation.

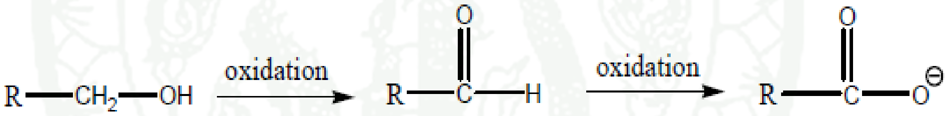

$$R-CH_2-OH \xrightarrow{\text{oxidation}} R-\overset{O}{\overset{\|}{C}}-H \xrightarrow{\text{oxidation}} R-\overset{O}{\overset{\|}{C}}-O^{\ominus}$$

C=O or COO^- group could increase the adsorption capacity of BAC because of its negative properties. Thus, it could attract a positive species such as metal ion or cationic molecules. The other oxidation reaction between charcoal and HNO_3 were shown in figure 21.

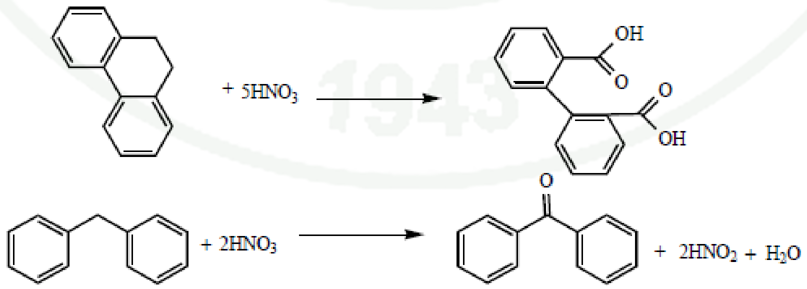

Figure 21 The formation of acidic functional groups by nitric acid reaction with thermal treatment.

Source: Wenzhong *et.al.* (2008)

2. Adsorption properties of BC and BAC

2.1 Cr(III) adsorption

2.1.1 Effect of Cr(III) dose

In this study, chromium solution condition was Cr(III) 5.00 mg/L in the volume of 25.00 mL, agitation speed 200 rpm at pH 5.01 (CH_3COOH – CH_3COONa buffer) and contact time for 3 hour. The dependence of Cr(III) adsorption on dose was studied by varying the amount of BC and BAC from 0.4 to 10.0 g/L by setting other parameters (pH, agitation speed and contact time) constant. Figure 22 and 23 show effect of Cr(III) dose on the removal efficiency of BC and BAC respectively.

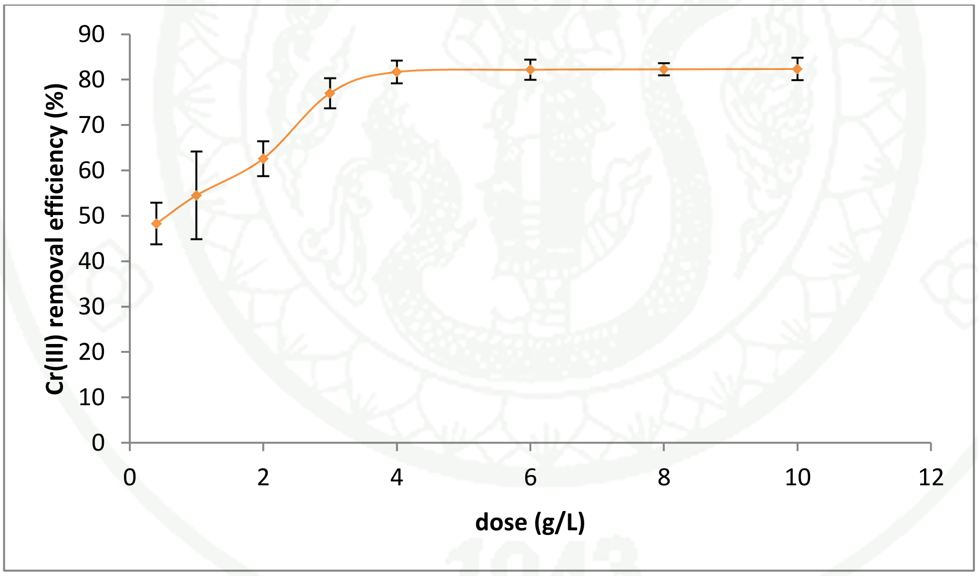

Figure 22 Effect of Cr(III) dose on the removal efficiency of BC (initial concentration of Cr(III) was 5 mg/L).

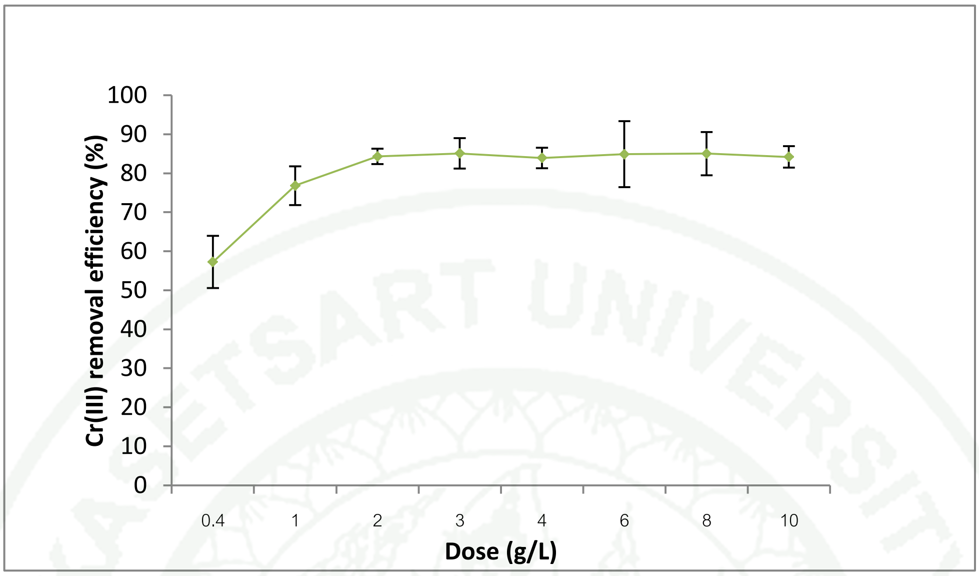

Figure 23 Effect of Cr(III) dose on the removal efficiency of BAC BC (initial concentration of Cr(III) was 5 mg/L)**.**

From figure 23, it can be observed that removal efficiency of BAC was improved with the increasing of Cr(III) dose up to a certain value. For 5 mg/L of Cr(III) concentration, the Cr (III) removal efficiency significantly increased from 57% to 84%, when the dose of BAC was increased from 0.4 to 2.0 g/L and Cr(III) removal efficiency of BC was increased from 48% to 81% when the dose of BC was increased from 0.4 to 4.0 g/L. The maximum Cr(III) removal efficiency of BC and BAC were 81.67 ± 2.51% and 84.31±1.99% respectively.

Cr(III) dose was defined as number of weight of charcoal in gram in the Cr(III) solution 1 liter at fixed concentration. That mean the lower dose had the higher adsorption capacity. In this research, BAC had lower Cr(III) dose than BC, because the activation with nitric increased the adsorption capacity of charcoal then the lower weight of BAC was used. It can be explained the fact that the higher the dose of adsorbent in the solution, the greater the availability of exchangeable sites for metal ions.

Nitric acid treatment increased the negative surface charge of bamboo charcoal, which is a favorable condition for Cr(III) removal. Thus, the negative surface charge of BAC started to acquire more positive charge of Cr(III) ions, make the situation electrostatically favorable for a higher Cr(III) uptake. It is suggested that the formation of C=O groups on the surface of BAC due to nitric acid treatment enhanced its adsorption affinity, that make more Cr(III) adsorption and pore diffusion.

2.1.2 Effect of pH

The Cr(III) removal efficiency was also studied as a function of contact time, agitation speed and optimum condition of dose (Cr(III) solution condition was Cr(III) 5.00 mg/L in the volume of 25.00 mL, agitation speed 200 rpm and 0.01 M of CH_3COOH – CH_3COONa buffer) and contact time for 3 hour dose for BC and BAC are 4.0g/L and 2.0 g/L respectively).

The optimum pH is very important, because pH affects not only the surface charge of adsorbent, but also the degree of ionization and speciation of adsorbate during the reaction. To examine the effect of pH on the Cr(III) removal efficiency, the pH of solution was varied from 3.0 to 6.0. The results are shown in figure 24 and 25.

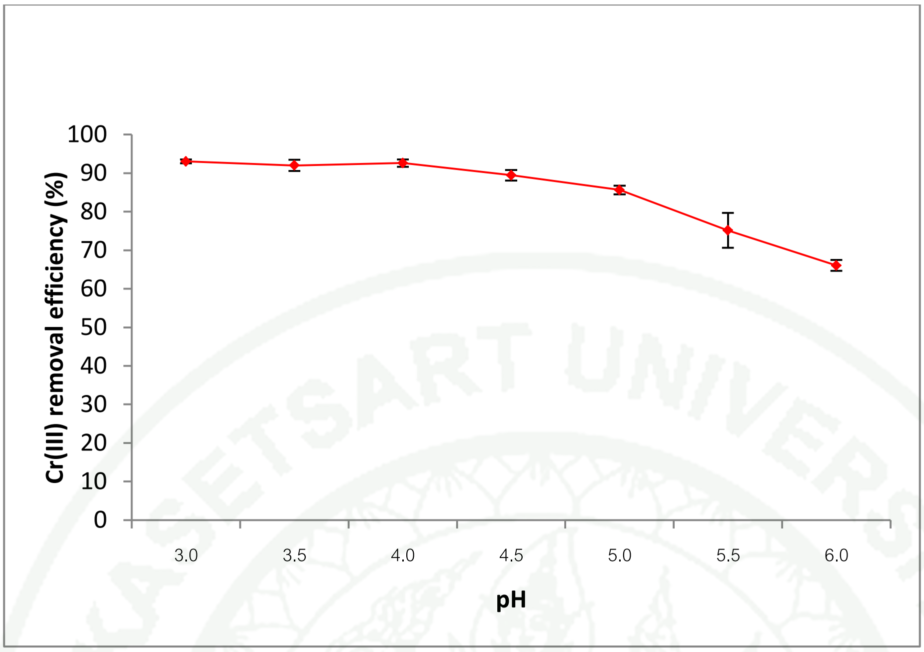

Figure 24 Effect of pH on the removal efficiency of BC (initial concentration of Cr(III) was 5 mg/L)**.**

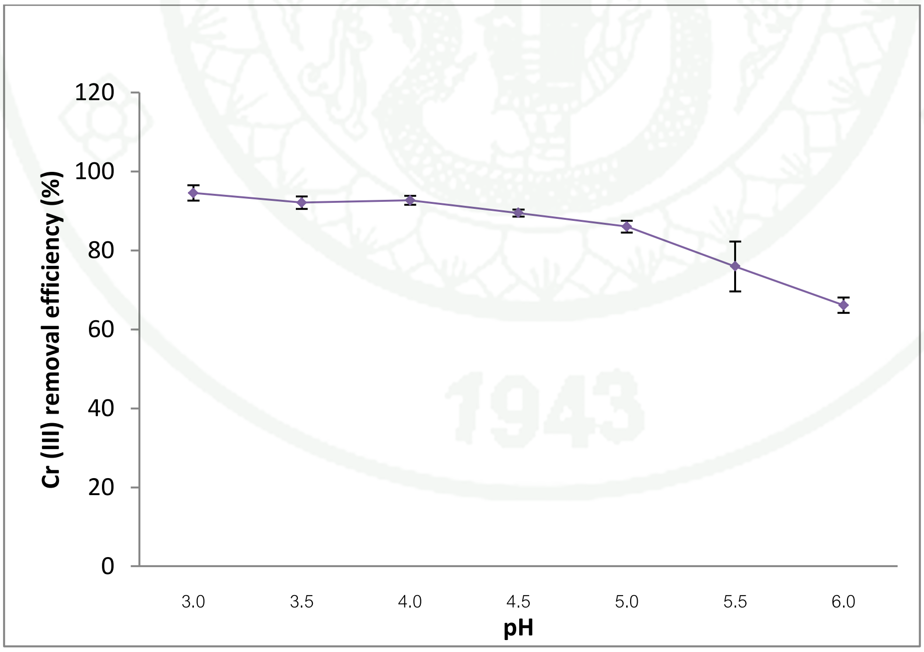

Figure 25 Effect of pH on the removal efficiency of BAC (initial concentration of Cr(III) was 5 mg/L)**.**

Figure 24 and 25 show that the Cr(III) removal efficiency of BC and BAC were slightly decreased as the pH increased from 4.5 to 6.0. In fact, the Cr(III) removal efficiency of both BC and BAC were stable over pH range of 3.0–4.0. This phenomenon can be attributed to the fact that a lower pH increases the negatively charged groups on the surface of charcoal, which leads to higher Cr uptake. It was found that there was a significant decreasing in Cr(III) adsorption for both of BC and BAC from 89% to 66% when pH of solution was increased from 4.5 to 6.0, due to the fact that the covalent coordination bonds between Cr(III) ions and the surface functional group of charcoal, such as carboxylic and hydroxyl, are very weak in basic condition. The maximum Cr(III) removal efficiency of BC and BAC at optimum pH (optimum pH was 4.0 on both BC and BAC), were 92.61 ± 0.94% and 92.68 ± 0.87% respectively. The adsorption capacity of BC and BAC were 1.98 mg/g and 1.01 mg/g respectively.

It can be attributed to the fact that surface modification increased the acidic site of BAC. Consequently, more surface oxygenated complexes were formed on its carbon surface (Aggarwal *et al*., 1999). Cr(III) in aqueous solution forms different species at various pHs. The speciation diagram for Cr(III) can be obtained by using the following reactions and equilibrium constants (Selomulya *et al*., 1999):

$$Cr^{3+} + H_2O \leftrightarrow [Cr(OH)]^{2+} + H^+ \quad (\log K = -4)$$
$$Cr^{3+} + 2H_2O \leftrightarrow [Cr(OH)_2]^{+} + 2H^+ \quad (\log K = -9.65)$$
$$Cr^{3+} + 4H_2O \leftrightarrow [Cr(OH)]^{4-} + 4H^+ \quad (\log K = -27.4)$$
$$Cr^{3+} + 3H_2O \leftrightarrow Cr(OH)_{3(s)} + 3H^+ \quad (\log K = -12)$$

The first reaction generates $Cr(OH)^{2+}$and proton which provide the increasing in acidity of Cr(III) solution. If $Cr^{3+}$is adsorbed, the first reaction shift to the left, leading to the depletion of protons and hence a rise in pH. In contrast, if $Cr(OH)^{2+}$adsorbs onto the adsorbent, the reaction shift to the right and the solution becomes more acidic. However, pH of a solution may also change due to the release and/or uptake of protons. Thus, $Cr(OH)_2^+$ specie is dominant at pH values between 6 and 8 while $Cr(OH)^{2+}$ and Cr^{3+} predominant in more acidic conditions. $Cr(OH)^{4-}$and $Cr(OH)_{3(s)}$ are most likely to be found in alkaline water.

The studies were not performed more than pH 6.0 due to the possibility of Cr(III) precipitation. Rivera- Utrilla and Sanchez-Polo (2003) calculated the distribution of Cr(III) species in aqueous solutions at different pH values. At pH 2, almost all the Cr(III) existed as Cr^{3+}cation (hexahydrated), whereas at pH 12 it existed as $Cr(OH)^{4-}$anion. At pH 4.0, the predominant species were Cr^{3+} (61.16%), $Cr(OH)^{2+}$ (38.60%), and $Cr(OH)_2^+$ (38.24%). While at pH 6.0 the predominant species were $Cr(OH)^{2+}$ (60.61%) and $Cr(OH)_2^+$ (38.24%). The adsorption increases in the range 3.0-4.0. In this pH range, all Cr(III) species are cationic and the predominant interactions in the adsorption process must have been electrostatic. The maximum adsorption capacities were achieved in a pH range (3-4) which the carbon surface presented a negative charge and the Cr(III) species were cationic. Thus, the adsorption of Cr(III) is an attractive electrostatic interactions between the ionized acid sites on the activated carbon surface and the Cr(III) cations.

The acidic functional groups of both BC and BAC consisting of carboxylic, hydroxyl, and carbonyl, which present on its surface. It was assumed that the physicochemical interactions might occur which could be expressed as follows:

$$M^{n+} + n(\text{-COOH}) \longleftrightarrow (\text{-COO}^-)_nM + nH^+$$

Where;

(–COOH) represent the surface functional group of BC and BAC.

n is the coefficient of the reaction component, depending on the oxidation state of metal ions, M^{n+} and $H^+$are Cr (III) and hydrogen ions respectively.

Table 6 Adsorption capacities of BC, BAC and other adsorbents for the removal of Cr(III).

Activated carbons/adsorbents	Adsorption Capacity(mg/g)	References
BC	1.01	This studied
BAC	1.98	
Coconut shell-based activated carbon	2.00	Abdel *et al.* (2001)
Activated carbon oxidized with HNO_3 and heated at 873 °K in a N_2 flow for 2 h	0.2	Bautista-Toledo *et al.* (1994)
Activated carbon	2.7	
Activated carbon oxidized with HNO_3	25.3	
Activated carbon, ACF-310	3.52	Aggarwal *et al.* (1999)

Table 6 shows summery of various adsorbents previously studied for Cr(III) removal in term of adsorption capacity (mg/g). It was shows that BAC had an adsorption capacity near coconut shell-based activated carbon and activated carbon and Activated carbon. BC had a higher adsorption capacity than Activated carbon oxidized with HNO_3 and heated at 873 K in a N_2 flow for 2 hours.

2.2 Phenol adsorption

2.2.1 Moisture of charcoal

Two grams of BC and BAC were used to determined the moisture at the temperature of 110 ^{o}C. It is necessary to understand the moisture of BC and BAC which might related to the adsorption ability of charcoal. Also it must be used to calculate the phenol value. Moisture of BC and BAC are 2.55% and 0.19% respectively.

Abiko *et al.* (2010) found that, the increasing in moisture of charcoal decreased the adsorption capacity of charcoal with organic vapor due to the competition between the adsorption of water and other adsorbent.

2.2.2 Phenol value

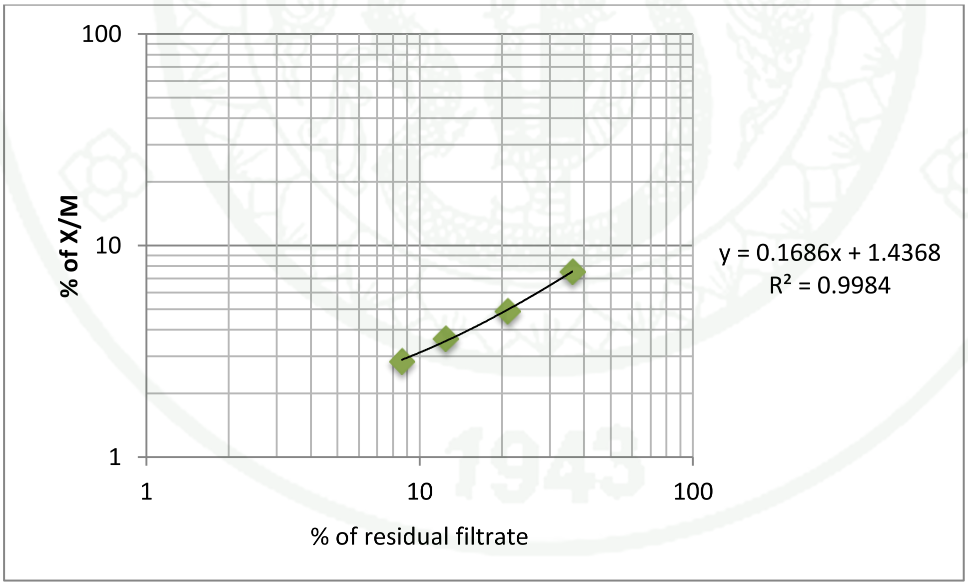

Figure 26 The relationship between the average of % of X/M and residual filtrate onto BC.

(X/M is the ratio of the adsorption phenol to amounts of charcoals)

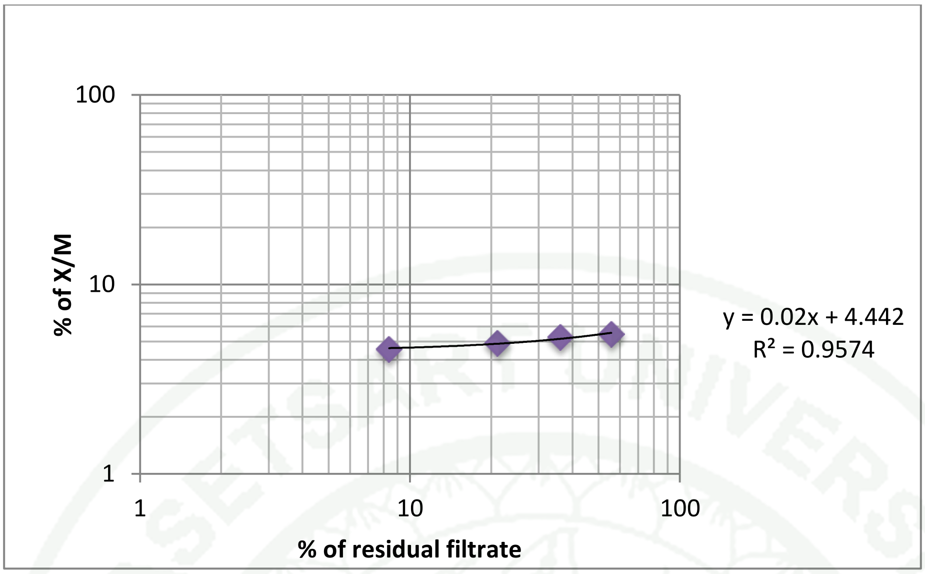

Figure 27 The relationship between the average of % of X/M and % of residual filtrate onto BAC.
(X/M is the ratio of the adsorption phenol to amounts of charcoals)

The relationship between the average of % of X/M and % of residual filtrate onto BC and BAC are shown in figure 26 and 27 respectively. The phenol value was the value which indicated the adsorption ability between adsorbent and phenol molecule. A low phenol value indicated the high adsorption ability. Based on this process, phenol value was calculated from the 10% remaining concentration from the initial phenol concentration, that the activated carbon adsorbed, by using aboved graph. Therefore, if the remaining concentration of phenol was minuted, the activated carbon should adsorb phenol with the high extent.

In this research, the phenol value was calculated follow by AWWA B600 test method, which defined as the concentration of activated carbon in grams per liter required to reduce standard phenol solution to 10%, that's mean the lower phenol value the higher adsorption capacity and the 5 mg/L of phenol was used as an initial concentration. The phenol values of BC and BAC for adsorption ability of phenol were 28.09±1.37 g/L and19.35 ± 0.08 g/L, respectively. Phenol value of BAC had significant difference from BC ($p \leq 0.05$; paired t-test). The adsorption capacity of BC and BAC, calculated form phenol value, were 0.19 mg/g and 0.26 mg/g, respectively. In this experiment, BC and BAC had higher phenol value than AWWA suggested (phenol value of activated carbon should be less than 3.5). That mean both of BC and BAC had low capability for phenol adsorption, because the preparation of activated carbon from chemical activation, causing C=O or COO^- functional groups on surface of activated carbon. The carboxylate groups on the carbon surface removed the π-electron from the activated carbon aromatic ring matrix, causing a decrease in the strength of interactions between the benzene ring of phenol and the carbon’s basal planes, which decreases the phenol uptake (Salame and Bandosz, 2003).

Mattson and Mark (1971), assigned the mechanism of phenol adsorption as being determined by so-called “π–π interactions” and “donor–acceptor complex” formation. The first factor assumes that oxygen atoms bonded to the carbon to reduce the π electron density and weaken the dispersion forces between phenol π electrons ring and the π electrons of carbons. The second one postulate that the adsorption mechanism is based on the formation of donor–acceptor complexes between the surface carbonyl groups (electron donors) and the aromatic rings of phenol acting as the acceptor, and the decrease in phenol adsorption after carbon oxidation due to the oxidation of surface carbonyls.

2.3 Adsorption equilibrium time of phenol onto BC and BAC.

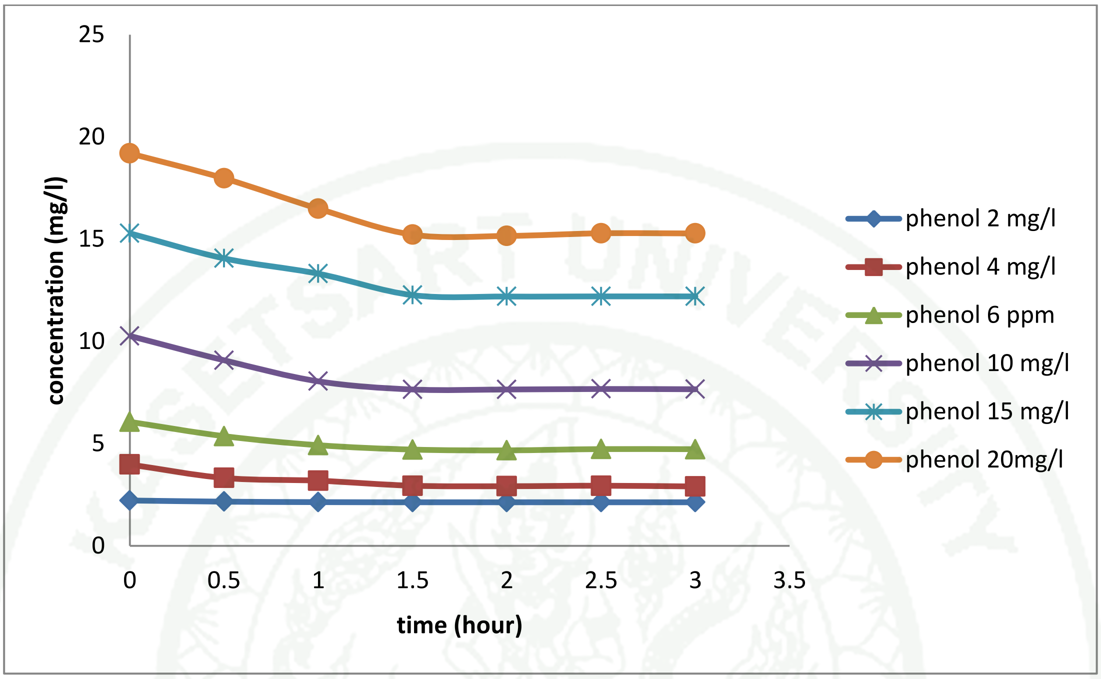

Figure 28 Adsorption equilibrium time of phenol onto BC.

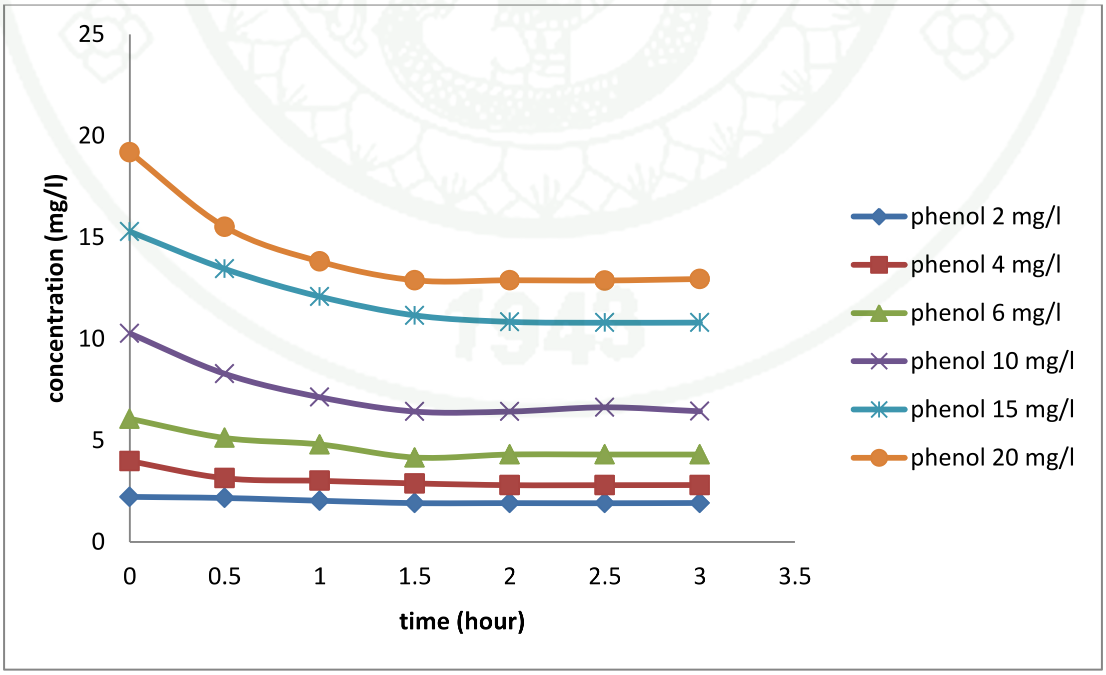

Figure 29 Adsorption equilibrium time of phenol onto BAC.

Figure 28 and 29 show the adsorption equilibrium time of BC and BAC. The phenol adsorption was also studied as a function of contact time (from 1 to 3 hour) and phenol concentration (25 ml of 2-20 mg/L phenol solution at pH 6.5 and 0.2 g of charcoal were used).

For BC and BAC, phenol concentrations were slightly decreased after adsorption occurred to reach equilibrium in the same time at 1.5 hour. Figure 28 and 29 show that there are three regions of phenol uptakes, in each straight line. The uptake rate is initially very fast, then medium and finally giving way to slow uptake. It is likely that the adsorbateis initially transported to macro-, then meso-, and finally slowly diffused into micropores.

2.2.3 Adsorption isotherms of phenol onto BC and BAC.

Figure 30-33 showed the Freundlich plots of log q_e versus log C_e and Langmuir plots of C_e/ q_e versus C_e for the adsorption of phenol onto the BC and BAC.

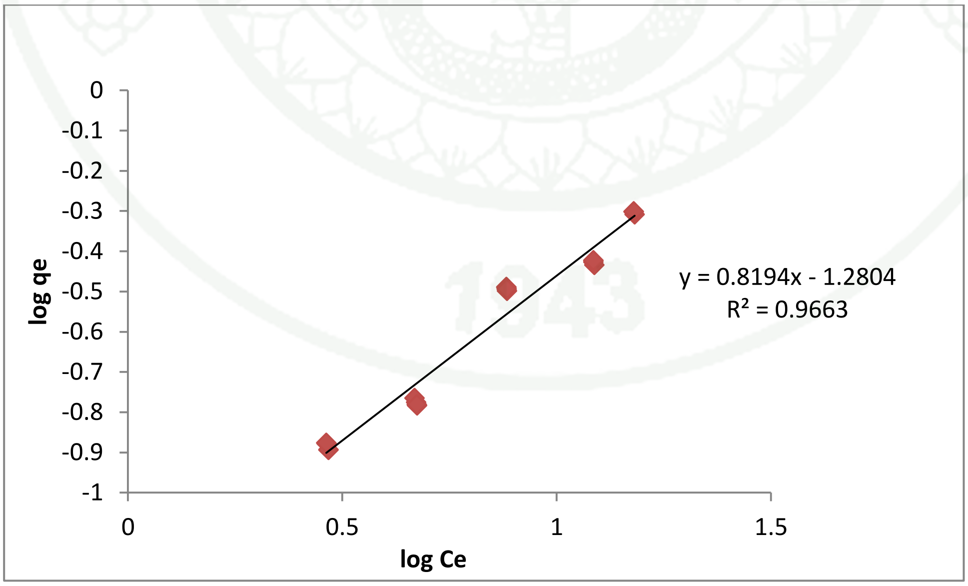

Figure 30 Freundlich adsorption isotherm of phenol onto BC.

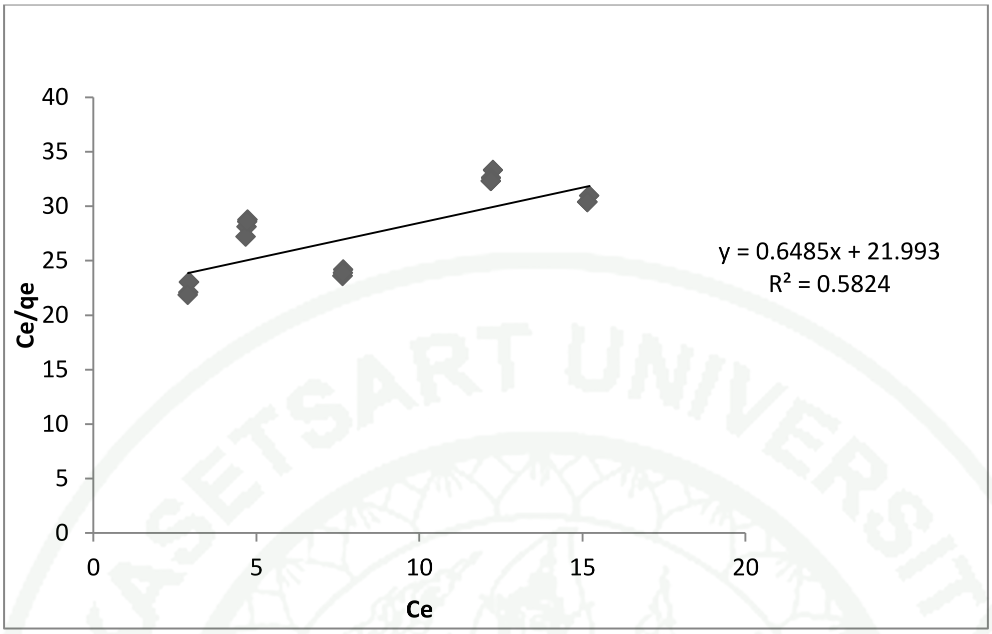

Figure 31 Langmuir adsorption isotherm of phenol onto BC.

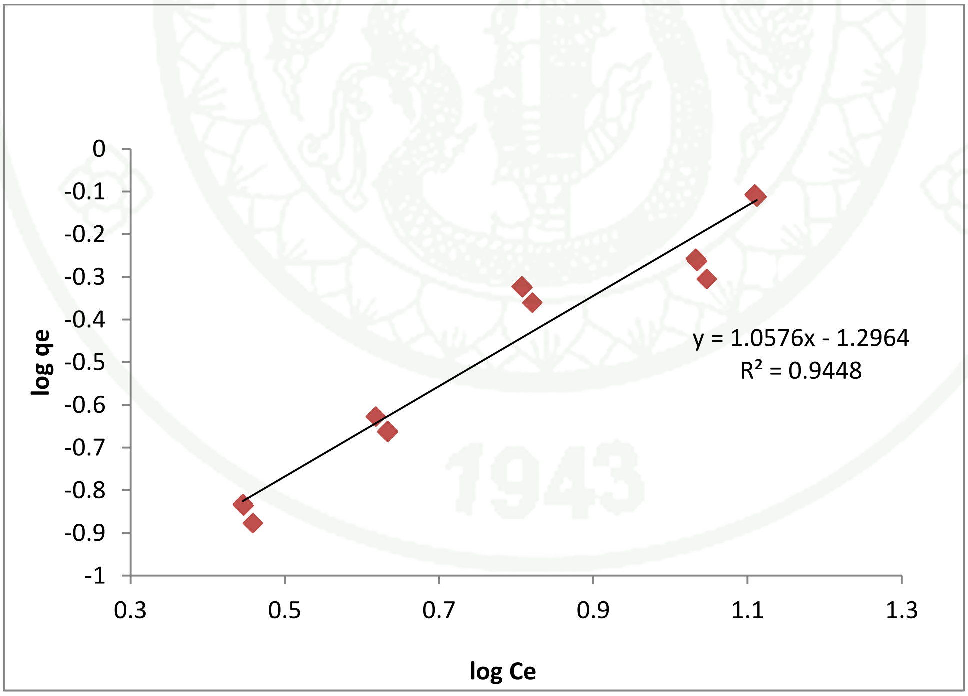

Figure 32 Freundlich adsorption isotherm of phenol onto BAC.

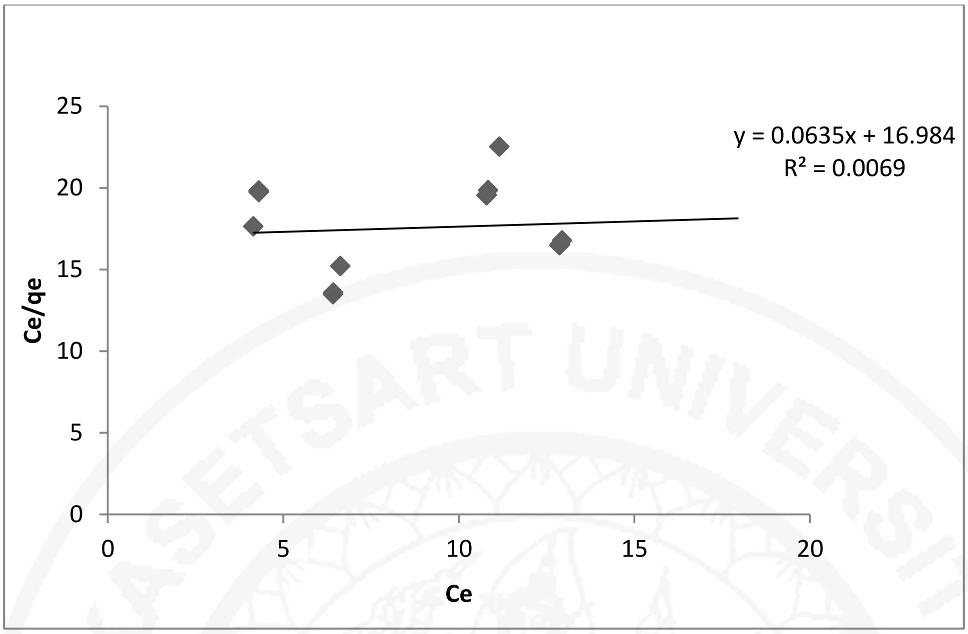

Figure 33 Langmuir adsorption isotherm of phenol onto BAC**.**

Table 7 Langmuir and Freundlich isotherm constants for phenol**.**

Charcoal	Langmuir isotherm			Freundlich isotherm		
	Q_o(mg/g)	b (L/mg)	R^2	1/n	k_F	R^2
BC	1.54	0.029	0.582	0.819	0.052	0.996
BAC	15.75	0.004	0.007	1.058	0.051	0.945

The adsorption isotherm indicates how the adsorption molecules distributed between the liquid phase and the solid phase, when the adsorption process reaches an equilibrium state. The analysis of the isotherm data by fitting them to different isotherm models is an important step to find the suitable model that can be used for design purpose (Guendi 1991). The Langmuir and Freundlich adsorption isotherm constants for phenol adsorption are given in table 7. The fitting to the Langmuir adsorption isotherm model was similar in comparison to the Freundlich model according to R^2 values.

A comparison in table 7 was also made between two isotherms plotted in figure 30-33 which showed the experimental data points and the two theoretical isotherms plotted on the same graph. As seen from table 7, the Freundlich model were better fit (R^2= 0.996 and 0.945 for BC and BAC respectively) than the Langmuir model (R^2= 0.582 and 0.007 for BC and BAC respectively). As also illustrated in table 7 the value of $1/n$ is 0.819 and 1.058 for BC and BAC respectively), which indicated favorable adsorption for BC but un favorable for BAC. Therefore, the types of adsorption could be either monolayer or multilayer coverage of phenol molecules onto surface of BC and BAC. The Freundlich constants showed that the all 1/n value were in the range of 0-1 indicated favorable multilayer adsorption of phenol (Hameed *et al.*, 2007). However, the k_F value of BC was higher than BAC, pointing out that the BC had high adsorption capacity. The Langmuir constant bands, $Q_{0,}$ were calculated from this isotherm and their values were given in table 7. The Langmuir constants showed that the Q_0 of BAC was higher than BC. Moreover, the b value of was BC higher than BAC. It was indicated that the BC had the higher adsorption energy than BAC.

2.2.4 Specific surface area for adsorption of phenol.

The specific surface area for adsorption of phenol onto BC and BAC were calculated by this equation;

$$S = \frac{Q_0}{MW} \text{x N x a} \qquad (9)$$

Where;

S = the specific surface area (m^2/g)

Q_o = the the maximum surface coverage (formation of monolayer) of sorbent (mg/g)

MW = the molecular weight (g/mol)

N = the Avogadro number ($6.02x10^{23}$molecule/mol)

a = the cross sectional area of adsorbate ($Å^2$)

For Phenol; MW = 94.11 g/mol, a = 52.2 $Å^2$

Table 8 The specific surface area of samples for adsorption of phenol**.**

Charcoal	specific surface area (m^2/g)
BC	5.14
BAC	52.59

According to the Langmuir isotherm in case of phenol, this pointed out the fact that the phenol adsorption was the mono-layered adsorption, in which the specific surface area could be calculated by replacing the Q_0 value as shown in table 7 on the equation 9. The obtained specific surface area of BC and BAC were in the range of 5-53 m^2/g. The specific surface area value reflected the phenol adsorption ability of the activated carbon, in that, the higher value, the more adsorption ability. In case of BC, it had the highest adsorption ability although its specific surface area was lower than the specific surface area of BAC which, due to the multi-layered adsorption on the surface area of BC.

Table 9 Adsorption capacities of BC, BAC and other adsorbents for the removal of phenol (at 90% phenol adsorbed).

Activated carbons/adsorbents	Phenol concentration (mg/L)	Dose (g/L)	Adsorption Capacity (mg/g)	References
BC	5	28.09	0.19	This studied
BAC		19.35	0.26	
lignite	-	-	10	Polat *et al.*(2006)

Table 9 (Continued)

Activated carbons/adsorbents	Phenol concentration (mg/L)	Dose (g/L)	Adsorption Capacity (mg/g)	References
activated carbon (AC)	30-50	10	-	Somnath *et al.* (2007)
Bagasse ash (BA)	30	15	1.8	
wood charcoal (WC)	50	60	0.75	

Table 9 shows summery of various adsorbents previously studied for phenol removal term of adsorption capacity (mg/g) and dose (g/L) at 90% phenol adsorbed. It was shows that, both of BC and BAC had very low adsorption capacity (0.19 mg/L and 0.26 mg/L respectively) compared to other adsorbent. The adsorption capacity of BAC shows that, the surface modification of nitric acid increased the adsorption capacity about 30%.

CONCLUSION AND RECOMMENDATION

Conclusion

From the result of proximate analysis properties, from the SEM result, the surface morphology of BAC had higher number of pores than BC. The increase of a number of pores resulted in the increasing of the adsorption surface area. However, the pore size of the activated carbon should have the appropriate size for each of the adsorbate as well. However BAC and BC had the same functional groups but more carbonyl groups was present on the activated carbon resulting from oxidation reaction, which was able to be seen in the IR results at 1,580 – 1,540 cm^{-1} (C=O) and 1200-1050 cm^{-1}(C-O). The occurrence of COO^- on the activated carbon surface had an impact on the adsorption efficiency. Nevertheless, the presence of C=O and COO^- groups on the activated carbon surface after activation brought about the decreasing of phenol adsorption ability.

BC and BAC had maximum Cr(III) removal efficiency stable from pH 3-4 and slightly decreased at pH 4.5, the maximum adsorption capacity of BC and BAC at pH 4 were 1.01 mg/g and 1.98 mg/g which could be removed Cr(III) 92.61±0.94% and 92.68±0.84% respectively. From the phenol adsorption, the phenol values of BC and BAC for adsorption ability of phenol were 28.09±1.37 g/L and19.35 ± 0.08 g/L and the adsorption capacity of BC and BAC, calculated form phenol value, were 0.19 mg/g and 0.26 mg/g, respectively.

BAC was appropriate to use as an adsorbent for Cr(III) removal because it had adsorption capacity nearly to the other activated carbon which has been reported. However, both BC and BAC were not prospered to use for phenol removal, because of the very low adsorption capacity compared to the other adsorbent which has been reported. The adsorption isotherm indicated that the adsorption mechanism of phenol of BC and BAC should be fitted with Freundlich isotherm model.

Recommendation

1. In the carbonization process, inert or N_2 atmosphere should be adopted instead of O_2 atmosphere because of the decreasing in the amount of ash from the oxidation process of bamboo wood and provide the larger amount of charcoal.

2. Both BC and BAC should be used for adsorption study in term of the adsorption ability of activated carbon after the first-time usage.

LITERATURE CITED

Aber, S., A. Khataee and M. Sheydaei. 2009. Optimization of activated carbon fiber preparation from Kenaf using K_2HPO_4 as chemical activator for adsorption of phenolic compounds. **Biores**.**Technol**. 100: 6586-6591.

Abiko, H., M. Furuse and T. Takano. 2010. Reduction of adsorption capacity of coconut shell activated carbon for organic vapors due to moisture contents. **Industrial Health** 48: 427–437.

Aggarwal, D., M. Goyal, and R.C. Bansal. 1999. Adsorption of chromium by activated carbon from aqueous solution. **Carbon** 37: 1989–1997.

Ahmad, A.A. and B.H. Hameed. 2009. Fixed-bed adsorption of reactive azo dye onto granular activated carbon prepared from waste. **J. Hazard. Mater.** 175: 298-303.

American Water Works Association. 1995. **Standard for Activated Carbon. AWWA B600-95**. United States of America.

Babel, S. and T.A. Kurniawan. 2004. Cr(VI) removal from synthetic wastewater using coconut shell charcoal and commercial activated carbon modified with oxidizing agents and/or chitosan. **Chemosphere** 54: 951–967.

Bansal, R.C. and M. Goyal. 2005. **Activated Carbon Adsorption**. 1st ed. CRC Press, New York.

Bautista-Toledo, I., J. Rivera-Utrilla, M.A. Ferro-Garc´ıa, C. Moreno-Castilla. 1994. Influence of the oxygen surface complexes of activated carbons on the adsorption of chromium ions from aqueous solutions: effect of sodium chloride and humic acid. **Carbon** 32: 93–100.

Berl, E. 1938. **Formation and Properties of Activated Carbon**. 1st ed. Royal Society of Chemistry, United State of America.

Chan, L.S., W.H. Cheung and G. McKay. 2008. Adsorption of acid dyes by bamboo derived activated carbon. **Desalination** 218: 304-312.

Chan, L.S., W.H. Cheung and S.J. Allen. 2009. Separation of acid-dyes mixture by bamboo derived active carbon. **Sep**. **Pur**. **Technol**. 67: 166-172.

Chand, R., T.Watari, K. Inoue, H. N.Luitel, T. Torikai and M.Yada. 2009. Chemical modification of carbonized wheat and barley straw using HNO_3 and the adsorption of Cr(III). **J. Hazard. Mater.** 167: 319-324.

Cheremisinoff, P.N. and A.C. Morresi. 1987. Carbon adsorption application. In P.N. Cheremisinoff and F. Ellerbusch (eds.), **Carbon Adsorption Handbook**. Michigan: Ann Arbor Science.

Culp, G.L. and R.L. Culp. 1974. **New Concepts in Water Purification**. 1st ed. Van Nostrand Reinhold Company, New York.

Dahbi, S., M. Azzi, N. Saib, M. de la Guardia, R. Faure and R. Durand. 2002. Removal of trivalent chromium from tannery waste waters using bone charcoal. **Anal. Bioanal. Chem.** 374: 540–546.

El-Guendi, M. 1991. Homogeneous surface diffusion model of basic dyestuffsonto natural clay in batch adsorbers. **Adsorpt. Sci. Technol.** 2: 217–225.

El-Hendawy, A.N.A., S.E. Samra and B.S. Girgis. 2001. Adsorption characteristics of activated carbons obtained from corncobs. **Colloids and Surfaces A: Physicochem. Eng.** 180: 209–221.

Ghosh, P.K. 2009. Hexavalent chromium [Cr(VI)] removal by acid modified waste activated carbons. **J. Hazard. Mater.** 171:116-122.

Hameed, B.H., A.T.M. Din and A.L. Ahmad. 2007. Adsorption of methylene blue onto
bamboo-based activated carbon: Kinetics and equilibrium studies. **J. Hazard. Mater.** 141: 819-825.

Huang, G., J. X. Shi and T.A.G. Langrish. 2009. Removal of Cr(VI) from aqueous solution using activated carbon modified with nitric acid. **Chem. Eng. J.** 152: 434-439.

International Network for Bamboo and Rattan. 2009. **Thyrisostachys regia.** Available Source: http://www.inbar.int/publication/txt/tr17/thyrsostachys/TH%20RE.htm, March 10, 2012.

Ip, A.W.M., J.P. Barford and G. McKay. 2008. Production and comparison of high surface area bamboo derived active carbons. **Biores.Technol.** 99: 8909–8916.

Ip, A.W.M., J.P. Barford and G. McKay. 2009. Reactive Black dye adsorption/desorption onto different adsorbents: Effect of salt, surface chemistry, pore size and surface area. **J. Colloid Interface Sci.** 337: 32-38.

Japan International Research Center for Agricultural Sciences.2010. **Thyrsostachys siamensis Gamble**. Available Source: http://www.jircas.affrc.go.jp/project/value_addition/Vegetables/100.html, March 10, 2012.

Kumar, A., S. Kumar, S. Kumar and D.V. Gupta. 2007. Adsorption of phenol and 4-nitrophenol on granular activated carbon in basal salt medium: Equilibrium and kinetics. **J. Hazard. Mater.** 147: 155-166.

Mattson, J.S. and H.B. Mark. 1971. **Activated Carbon – Surface Chemistry and Adsorption from Solution**. Marcel Dekker.

Mohamed, F.Sh., W.A. Khater and M.R. Mostafa. 2006. Characterization and phenols sorptive properties of carbons activated by sulphuric acid. **Chem. Eng. J.** 116: 47–52.

Mohan, D., K.P. Singh and V.K. Singh. 2006. Trivalent chromium removal from wastewater using low cost activated carbon derived from agricultural waste material and activated carbon fabric cloth. **J. Hazard. Mater.** B135: 280–295.

Mui, E.L.K., W.H. Cheung, M. Valix and G. McKay**.** 2010. Activatedcarbons from bamboo scaffolding using acid activation. **Sep**. **Pur**. **Technol**. 74: 213-218.

Natale, F.D., A. Lancia, A. Molino and D. Musmarra. 2007. Removal of chromium ions form aqueous solutions by adsorption on activated carbon and char. **J. Hazard. Mater.** 145: 381–390.

Özkaya, B. 2006. Adsorption and desorption of phenol on activated carbon and a comparison of isotherm models. **J. Hazard. Mater.** B129: 158–163.

Phan, N.H., S. Rio, C. Faur, L.L. Coq, P.L. Cloirec and T.H. Nguyen. 2006. Production of fibrous activated carbons from natural cellulose (jute, coconut) fibers for water treatment applications. **Carbon** 44: 2569-2577.

Podkościelny, P. and K. Nieszporek. 2007. Heterogeneity of activated carbons in adsorption of phenols from aqueous solutions—Comparison of experimental isotherm data and simulation predictions. **Appl. Surf. Sci.** 253: 3563–3570.

Polat, H., M. Molva and M. Polat. 2006. Capacity and mechanism of phenol adsorption on lignite. **Int. J. Miner. Process.** 79: 264–273.

Pollution Control Department. n.d. **Adsorption Process.** Available Source: http://www.pcd.go.th/info_serv/Datasmell/design_absorbtion.htm, March 10, 2012.

Rivera-Utrilla, J. and M. Sánchez-Polo. 2003. Adsorption of Cr(III) on ozonized activated carbon. Importance of C-π cation interactions. **Water research** 37: 3335-3340.

Salame, I.I. and T.J. Bandosz. 2003. Role of surface chemistry in adsorption of phenol on activated carbons. **J. Colloid Interface Sci.** 264: 307-312.

Saxena, P.B. n.d. **I.I.T. Chemistry**.Vol. I. Krishana Prakashan Media (p), Meerut.

Selomulya,C., V. Meeyoo and R. Amal. 1999 .Mechanisms of Cr(VI) removal from water by various types of activated carbons. **J. Chem. Technol. Biotechnol.** 74: 111–122.

Shen, W., Z. Li and Y. Liu. 2008. Surface Chemical Functional Groups Modification of Porous Carbon. **Chem**. **Eng**. 1:27-40.

Somnath M., S. Kumar, A.K. Misra and M. Fan. 2007. Removal of phenols from water environment by activated carbon, bagasse ash and wood charcoal. **Chem. Eng. J**. 129: 133-142.

Stavropoulos, G.G., P. Samaras and G.P. Sakellaropoulos. 2007. Effect of activated carbons modification on porosity, surface structure and phenol adsorption**. J. Hazard. Mater.** 151: 414-421.

Suzuki, M. 1990. **Adsorption engineering**. Chemical Engineering Monograps Vol. 25 Kodansha, Tokyo.

Tangjuank, S., N. Insuk, V. Udeye and J. Tontrakoon. 2009. Chromium (III) sorption from aqueous solutions using activated carbon prepared from cashew nut shells. **J. Phys. Sci**. 8: 412-417.

Tershkol, M.M. 1969. **Chemistry and Physics of Carbon**. 1st ed. Marcel Dekker, New York.

Terzyk, A.P. 2003. Further insights into the role of carbon surface functionalities in the mechanism of phenol adsorption. **J. Colloid Interface Sci.** 268: 301–329.

Wang, Y., C. Liu and Y. Zhou. 2008. Preparation and adsorption performances of mesopore-enriched bamboo activated carbon. **Front. Chem. Eng. China** 4: 473-477.

Wikipedia. 2012. **Activated carbon**. Available Source: http://www.wikipedia.org/wiki/activated _carbon, March 10, 2012.

________a. 2012. **Chromium**. Available Source: http://en.wikipedia.org/wiki/Chromium, March 10, 2012.

________b. 2012. **Phenol**. Available Source: http://en.wikipedia.org/wiki/Phenol, March 10, 2012.

________c. 2007. **Phenol 3D Structure**. Available Source: http://en.wikipedia.org/wiki/File:Phenol-3D-balls.png#file, March 10, 2012.

________d. 2012. **Pore size**. Available Source: http://www.iitk.ac.in/newhtml/storyoftheweek52.htm, March 10, 2012.

APPENDICES

Appendix A

Standard Test Method for Determination of Phenol Value of Activated Carbon

AWWA B600

APPENDIX B

Phenol and Tannin Values

This appendix is for information only and is not a part of AWWA B600.

Section B.1 Phenol Value

Sec. B.1.1 Phenol Value Test

The phenol value test procedure from ANSI/AWWA B600-78 is reprinted below for the information of ANSI/AWWA B600-96 users. ANSI/AWWA B600-78 stated, "Unless otherwise specified by the purchaser, the phenol value of the activated carbon shall not be greater than 3.5." The modified phenol value used in this standard is defined as the concentration of activated carbon in grams per litre required to reduce the standard phenol concentration from 200 mg/L to 20 mg/L.

Sec. B.1.2 Reagents and Equipment

a. Stock phenol solution. Dissolve 1 g of reagent-grade phenol in distilled water and dilute to 1 L. Phenol should be weighed on a glass weighing dish. Rinse the weighing dish with distilled water several times to ensure the removal of all phenol from the weighing dish into the solution. The solution need not be buffered. Standardize the solution. After two weeks, the solution should be discarded and a new solution prepared. (Reagent-grade phenol must be stored in a refrigerator.)

b. Sodium thiosulfate, 0.1*N*. Dissolve 25 g of reagent-grade sodium thiosulfate and 1 g of reagent-grade sodium carbonate, as a preservative, in boiled distilled water, and make up to 1 L. Store in a brown bottle. Standardize the solution.

c. Sodium thiosulfate, 0.01*N*. Dilute 100 mL of the standardized 0.1*N* sodium thiosulfate solution to 1 L with boiled distilled water. Store in a brown bottle. Standardize the solution.

d. Potassium bromate–bromide, 0.1*N*. Dissolve 2.784 g of reagent-grade potassium bromate and 10 g of reagent-grade potassium bromide (bromate-free) in distilled water, and dilute to 1 L. Store in a brown bottle.

e. Potassium biniodate, 0.1*N*. Dissolve 3.250 g of potassium biniodate, primary standard, in distilled water, and make up to 1 L.

f. Potassium biniodate, 0.025*N*. Dissolve 0.8125 g of potassium biniodate, primary standard, in distilled water, and make up to 1 L.

g. Potassium iodide, 12.5 percent. Dissolve 25 g of reagent-grade potassium iodide in 175 mL of distilled water and dilute to 200 mL. Store solution in a brown bottle in a dark place.

h. Starch solution. Dissolve 2.5 g of soluble potato-powder starch and 1.25 g of reagent-grade salicylic acid in 50 mL of distilled water. Add the dissolved starch and salicylic acid slowly, while stirring, to 950 mL of boiling distilled water. Rinse the 150-mL beaker with some of the hot starch solution to ensure removal of all of the starch.

i. Buffer solution, 8 strength. Dissolve 728 g of anhydrous disodium phosphate (Na_2HPO_4), or equivalent weight of crystalline phosphate, in 2 L of hot distilled water. When the phosphate is completely dissolved, acidify with about 100 mL of concentrated reagent-grade phosphoric acid and make up to 7 L. Make final adjustment to pH 6.5 ± 0.1.

Sec. B.1.3 Standardization of Reagents

The standardization of reagents follows:

a. **Sodium thiosulfate.** Add 100 mL of distilled water, 4 mL of concentrated reagent-grade hydrochloric acid, and 8 mL of 12.5 percent potassium iodide solution to a 500-mL iodine flask and mix. Rinse the sides of the flask with distilled water.

When standardizing $0.1N$ sodium thiosulfate solution, add 25 mL of $0.1N$ potassium biniodate solution.

When standardizing $0.01N$ sodium thiosulfate solution, add 10 mL of $0.025N$ potassium biniodate solution.

Using a transfer pipette, add the potassium biniodate solution to the flask. Mix and allow to stand for 3 min. Titrate with the sodium thiosulfate solution, using starch as the indicator.

$$\text{normality sodium thiosulfate solution} = \frac{\text{millilitre potassium biniodate solution} \times \text{normality factor}}{\text{millilitre sodium thiosulfate solution used}}$$

b. **Stock phenol solution.** Pipette 25 mL of stock phenol solution into a 500-mL iodine flask. Using a pipette or a burette, add 25 mL of $0.1N$ potassium bromate–bromide solution. Shake flask. Add 5 mL of concentrated hydrochloric acid. After 3 min, add 8 mL of 12.5 percent potassium iodide solution. Allow to stand for 3 min and titrate the liberated iodine with $0.1N$ sodium thiosulfate solution, using starch solution as the indicator.

$$\text{concentration of phenol (grams per litre)} = \frac{\begin{bmatrix}(\text{millilitre bromate–bromide} \times \text{normality factor}) - \\ (\text{millilitre sodium thiosulfate} \times \text{normality factor})\end{bmatrix}}{\text{millilitre stock phenol solution}} \times 15.685$$

Sec. B.1.4 Phenol Test Procedure

The phenol test procedure follows:

a. Prepare a test phenol solution with a concentration of 200 mg/L of phenol by diluting one volume of stock phenol solution (1,000 mg/L) with four volumes of single-strength buffer solution. Single-strength buffer solution is prepared by diluting one volume of 8-strength buffer solution with seven volumes of distilled water. For example, to prepare 1 L of test phenol solution use 200 mL of stock phenol solution and 800 mL of single-strength buffer solution (100 mL of 8-strength buffer solution plus 700 mL of distilled water.) If the stock phenol solution is not of the exact concentration (1 g/L), adjust the volume used so that the test solution is maintained at 200 mg/L of phenol.

When preparing test phenol solution, prepare enough to conduct all of the sample for the day. A four-point isotherm for a single activated carbon requires 800 mL of test phenol solution 200 mL for each activated carbon dosage). It is advisable to make up some solution in excess of the amount required to allow for spillage, and so forth.

b. Use the activated carbon as received, and determine the moisture content according to Sec. 5.2.3 of ANSI/AWWA B600.

Use four dosages for each activated carbon. At least one dosage should adsorb 90 percent or more of the phenol in the test phenol solution. Activated carbon weights of 0.4 g, 0.5 g, 0.6 g, and 0.7 g are usually satisfactory. If these weights do not give the desired range of phenol adsorption, higher or lower weights may be used. Each activated carbon dosage is weighed into an Erlenmeyer flask.

c. Using pipette, add 200 mL of test phenol solution (200 mg/L of phenol) to each Erlenmeyer flask. Add only about 100 mL of solution initially to thoroughly wet the activated carbon, and rinse the sides of the flask with the remaining portion. Close the flasks with rubber caps and place them in an Eberback Water Bath Shaker (or equivalent) at ambient temperature, without water in the bath, and shake for 30 min. Samples are to be filtered by gravity using Whatman No. 2V, 24-cm fluted paper (or equivalent) on a 5-in. (127-mm) funnel. Allow the samples to filter completely.

Sec. B.1.5 Residual Phenol Determination

Determine the residual phenol concentration for each activated carbon treated filtrate by either the titration method or the spectrophotometric method according to the following procedures:

a. Titration method. Transfer a 150-mL portion of each filtrate, measured with a graduated cylinder, to a 500-mL iodine flask. Add 10 mL of concentrated, reagent-grade hydrochloric acid to each flask.

Add from a burette 0.1*N* potassium bromate–bromide solution until a light yellow color develops, indicating that an excess has been added. Replace the stopper immediately, shake the flask vigorously for a few seconds, and then place the flask in cold water. The potassium bromate–bromide solution should be added as quickly as possible so that the liberated bromine does not escape. Record the potassium bromate–bromide titration.

Place the flasks in a sink with a stoppered drain or in a cold-water bath, with cold tap water running into it to cool the flasks. Keep the water as cold as possible, taking care not to fill the sink, causing the flasks to upset. After the flasks are cooled, add 12.5 percent potassium iodide solution to the flange top of the flask. Completely fill the top. Loosen the stopper to allow the potassium iodide solution to be drawn into the flask by the vacuum. Immediately drop the stopper back into place. (The flask-cooling period must be adequate to develop the required vacuum. If multiple activated carbons are tested, add potassium bromate–bromide solution to at least eight of the samples, and then add the potassium iodide to the first four samples, while allowing the last four samples to cool.) After the potassium iodide solution has been drawn into the flask, rinse the top of the flask (using a wash bottle) with distilled water. Loosen the stopper and allow the water to run into the flask, rinsing all the potassium iodide into the flask. Remove the flasks from the cold water. Titrate the liberated iodine with 0.01*N* sodium thiosulfate solution, using starch as the indicator. Record the sodium thiosulfate titration.

$$\text{residual phenol (milligram per litre)} = \begin{bmatrix} \text{(millilitre bromate–bromide} \times \text{normality factor)} - \\ \text{(millilitre sodium thiosulfate} \times \text{normality factor)} \end{bmatrix} \times 104.6$$

b. Spectrophotometric method. Prepare 1,500 mL of buffer solution mixture by adding one volume of 8-strength buffer solution to nine volumes of distilled water. The buffer solution mixture is used as the reference solution in the spectrophotometer and as the diluent in preparing the standard phenol reference curve.

Prepare standards containing 20 mg/L, 40 mg/L, 60 mg/L, 80 mg/L, 100 mg/L, and 120 mg/L phenol. To make these standards, measure from a burette 4 mL, 8 mL, 12 mL, 16 mL, 20 mL, and 24 mL of stock phenol solution (1,000 mg/L), respectively, into 200-mL volumetric flasks. Dilute each to exactly 200 mL with the buffer solution mixture and mix thoroughly.

The optical density of each filtrate and each dilution of the standard phenol reference curve is read on the spectrophotometer at a wavelength of 270 µm using silica cells with a 10-mm light path. Buffer solution mixture is used as the reference to balance the spectrophotometer.

Plot the data for the phenol reference curve, milligram per litre phenol versus optical density, on arithmetic paper.

Determine the residual phenol concentration milligram per litre for each activated carbon treated filtrate from the phenol reference curve.

NOTES. The following notes list some aids for more accurate results when using a spectrophotometer:

1. Let the instrument warm up sufficiently before balancing it.
2. Be sure that no foreign particles or air bubbles are present in the cell.
3. Dry the cells thoroughly and polish with lens tissue.
4. Always use the same matched cell for the reference cell.
5. Rinse the cells thoroughly with distilled water.
6. Avoid making fingerprints on the cell face while placing the cell in the instrument.

Sec. B.1.6 Calculations

a. Determine the percentage of residual filtrate normality (remaining phenol) (see B600-78, Table 1, page 8) in each activated carbon treated filtrate:

$$\%\text{ of residual filtrate normality} = \frac{\text{milligram per litre residual phenol} \times 100}{200\ (\text{milligram per litre phenol in test solution})}$$

b. Determine percentage of X (adsorbed phenol):

$$\%\text{ of } X = 100 - \%\text{ of residual filtrate normality}$$

c. Activated carbon dosages, per 200 mL of phenol solution, are multiplied by 5 to obtain activated carbon dosage, M, as grams per litre.

d. Calculate the percentage of X/M value for each activated carbon dosage.

e. Plot isotherm: percentage of residual filtrate normality on abscissa and percentage of X/M on ordinate on 2 × 2 cycle logarithmic paper and draw best straight line through the points.

f. Determine the percentage of X/M at 10 percent of residual filtrate normality.

g. Phenol value in grams per litre =

$$\frac{90}{\%\text{ of } X/M \text{ in grams per litre at } 10\%\text{ of residual filtrate normality}} \times \frac{100\% - \%\text{ of moisture}}{100\%}$$

As shown, this formula is on a dry activated carbon basis.

Appendix B

Adsorption results

Appendix Table A1 The concentration of Cr(III) at various amount of BC for effect of dose at Cr(III) 5 mg/L.

Replication	Dose (g/L)	BC weight (g)	Initial conc. (mg/L)	Final conc. (mg/L)	Removal efficiency (%)
1	0.4	0.0121	4.184	2.110	49.57
	1.0	0.0265		1.824	56.41
	2.0	0.0512		1.619	61.30
	3.0	0.0751		0.991	76.31
	4.0	0.1018		0.774	81.50
	6.0	0.1458		0.787	81.19
	8.0	0.2170		0.759	81.86
	10.0	0.2487		0.712	82.98
2	0.4	0.0120	5.068	2.579	49.11
	1.0	0.0255		2.533	50.02
	2.0	0.0503		1.809	64.31
	3.0	0.0730		1.210	76.12
	4.0	0.1019		0.975	80.76
	6.0	0.1582		0.892	82.40
	8.0	0.2037		0.909	82.06
	10.0	0.2546		0.871	82.81
3	0.4	0.0113	4.650	2.503	46.17
	1.0	0.0251		1.996	57.08
	2.0	0.0512		1.759	62.17
	3.0	0.0742		0.998	78.54
	4.0	0.1048		0.802	82.75
	6.0	0.1547		0.794	82.92
	8.0	0.2002		0.796	82.88
	10.0	0.2578		0.875	81.18

Appendix Table A2 The concentration of Cr(III) at various amount of BAC for effect of dose at Cr(III) 5 mg/L.

Replication	Dose (g/L)	BAC weight (g)	Initial conc. (mg/L)	Final conc. (mg/L)	Removal efficiency (%)
1	0.4	0.0130	4.184	1.671	60.06
	1.0	0.0267		0.874	79.11
	2.0	0.0517		0.619	85.21
	3.0	0.0781		0.551	86.83
	4.0	0.1018		0.654	84.37
	6.0	0.1488		0.787	81.19
	8.0	0.2170		0.519	87.60
	10.0	0.2487		0.712	82.98
2	0.4	0.0120	5.068	2.179	57.00
	1.0	0.0255		1.213	76.07
	2.0	0.0513		0.809	84.04
	3.0	0.0760		0.821	83.80
	4.0	0.1009		0.875	82.73
	6.0	0.1586		0.612	87.92
	8.0	0.2057		0.809	84.04
	10.0	0.2566		0.751	85.18
3	0.4	0.0113	4.650	2.107	54.69
	1.0	0.0257		1.146	75.35
	2.0	0.0512		0.759	83.68
	3.0	0.0772		0.713	84.67
	4.0	0.1048		0.712	84.69
	6.0	0.1549		0.674	85.51
	8.0	0.2022		0.769	83.46
	10.0	0.2578		0.725	84.41

Appendix Table A3 The concentration of Cr(III) at various pH for effect of dose on BC 0.1 g in Cr(III) 5 mg/L.

Replication	pH	Initial conc. (mg/L)	Final conc. (mg/L)	Removal efficiency (%)
1	3.0	4.261	0.307	92.80
	3.5	4.370	0.379	91.33
	4.0	4.392	0.317	92.78
	4.5	4.440	0.457	89.71
	5.0	4.273	0.626	85.35
	5.5	4.263	1.060	75.13
	6.0	4.385	1.447	67.00
2	3.0	4.261	0.295	93.08
	3.5	4.370	0.339	92.24
	4.0	4.392	0.313	92.87
	4.5	4.440	0.496	88.83
	5.0	4.273	0.591	86.17
	5.5	4.263	0.982	76.96
	6.0	4.385	1.500	65.79
3	3.0	4.261	0.291	93.17
	3.5	4.370	0.330	92.45
	4.0	4.392	0.344	92.17
	4.5	4.440	0.451	89.84
	5.0	4.273	0.622	85.44
	5.5	4.263	1.136	73.35
	6.0	4.385	1.521	65.31

Appendix Table A4 The concentration of Cr(III) at various pH for effect of dose on BAC 0.05 g in Cr(III) 5 mg/L.

Replication	pH	Initial conc. (mg/L)	Final conc. (mg/L)	Removal efficiency (%)
1	3.0	4.261	0.259	93.92
	3.5	4.370	0.377	91.37
	4.0	4.392	0.307	93.01
	4.5	4.440	0.457	89.71
	5.0	4.273	0.626	85.35
	5.5	4.263	1.056	75.23
	6.0	4.385	1.447	67.00
2	3.0	4.261	0.195	95.42
	3.5	4.370	0.327	92.52
	4.0	4.392	0.313	92.87
	4.5	4.440	0.486	89.05
	5.0	4.273	0.581	86.40
	5.5	4.263	0.906	78.75
	6.0	4.385	1.500	65.79
3	3.0	4.261	0.243	94.30
	3.5	4.370	0.331	92.43
	4.0	4.392	0.344	92.17
	4.5	4.440	0.461	89.62
	5.0	4.273	0.582	86.38
	5.5	4.263	1.116	73.82
	6.0	4.385	1.510	65.56

Appendix Table A5 Phenol value of BC.

Replication	BAC weight (g)	Residual concentration (mg/L)	% of residual concentration	% of X	M	% of X/M
1	0.2159	2.10	36.10	63.90	8.64	7.40
	0.4011	1.24	21.30	78.70	16.04	4.91
	0.5991	0.74	12.70	87.30	23.96	3.64
	0.8037	0.50	8.5669	91.43	32.15	2.84
2	0.2033	2.12	36.45	63.55	8.13	7.82
	0.4023	1.22	20.94	79.06	16.09	4.91
	0.6011	0.73	12.51	87.49	24.04	3.64
	0.8019	0.53	9.03	90.97	32.08	2.84
3	0.2140	2.10	36.05	63.95	8.56	7.47
	0.4036	1.22	20.92	79.08	16.14	4.90
	0.6024	0.71	12.16	87.84	24.10	3.65
	0.8043	0.48	8.27	91.73	32.17	2.85

Initial phenol concentration = 5.8221 mg/L

Appendix Table A6 Phenol value of BAC.

Replication	BAC weight (g)	Residual concentration (mg/L)	% of residual concentration	% of X	M	% of X/M
1	0.2023	3.14	55.61	44.39	8.09	5.49
	0.3020	2.05	36.33	63.67	12.08	5.27
	0.4039	1.17	20.78	79.22	16.16	4.90
	0.5067	0.46	8.06	91.94	20.27	4.54
2	0.2011	3.16	55.92	44.08	8.04	5.48
	0.3053	2.00	35.44	64.55	12.21	5.29
	0.4021	1.21	21.43	78.57	16.08	4.89
	0.5020	0.49	8.60	91.40	20.08	4.55
3	0.2020	3.14	55.66	44.34	8.08	5.49
	0.3016	2.06	36.53	63.47	12.06	5.26
	0.4033	1.19	21.14	78.86	16.13	4.89
	0.5039	0.48	8.45	91.55	20.16	4.54

Initial phenol concentration = 5.6491 mg/L

Appendix Table A7 The influence concentration of phenol at various time of BC for adsorption equilibrium time.

Initial conc. (mg/L)	Time (h)	BC weight (g)	C_e (mg/L)
2.21	0.5	0.2020	2.16
	1.0	0.2021	2.14
	1.5	0.2022	2.13
	2.0	0.2024	2.13
	2.5	0.2022	2.13
	3.0	0.2020	2.13
3.98	0.5	0.2031	3.32
	1.0	0.2022	3.18
	1.5	0.2032	2.94
	2.0	0.2011	2.91
	2.5	0.2030	2.94
	3.0	0.2022	2.90
6.06	0.5	0.2020	5.36
	1.0	0.2030	4.92
	1.5	0.2024	4.70
	2.0	0.2029	4.67
	2.5	0.2024	4.73
	3.0	0.2022	4.72
10.26	0.5	0.2053	9.07
	1.0	0.2019	8.04
	1.5	0.2021	7.64
	2.0	0.2024	7.64
	2.5	0.2046	7.67
	3.0	0.2033	7.66

Appendix Table A7 (Continued).

Initial conc. (mg/L)	Time (h)	BC weight (g)	C_e (mg/L)
15.28	0.5	0.2043	14.06
	1.0	0.2056	13.31
	1.5	0.2055	12.26
	2.0	0.204	12.19
	2.5	0.2063	12.20
	3.0	0.2044	12.20
19.19	0.5	0.2019	17.97
	1.0	0.2021	16.48
	1.5	0.2023	15.21
	2.0	0.2024	15.15
	2.5	0.2022	15.28
	3.0	0.2022	15.28

Appendix Table A8 The influence concentration of phenol at various time of BAC for adsorption equilibrium time.

Initial conc. (mg/L)	Time (h)	BAC weight (g)	C_e (mg/L)
2.21	0.5	0.2020	2.16
	1.0	0.2023	2.02
	1.5	0.2023	1.91
	2.0	0.2024	1.91
	2.5	0.2022	1.90
	3.0	0.2022	1.91
3.98	0.5	0.2034	3.14
	1.0	0.2022	3.01
	1.5	0.2072	2.87
	2.0	0.2011	2.79
	2.5	0.2020	2.79
	3.0	0.2021	2.80
6.06	0.5	0.2020	5.12
	1.0	0.2030	4.80
	1.5	0.2024	4.15
	2.0	0.2029	4.30
	2.5	0.2024	4.30
	3.0	0.2020	4.30
10.26	0.5	0.2053	8.28
	1.0	0.2032	7.12
	1.5	0.2021	6.41
	2.0	0.2024	6.41
	2.5	0.2086	6.63
	3.0	0.2023	6.43

Appendix Table A8 (Continued).

Initial conc. (mg/L)	Time (h)	BC weight (g)	C_e (mg/L)
15.28	0.5	0.2073	13.44
	1.0	0.2056	12.08
	1.5	0.2083	11.15
	2.0	0.2038	10.83
	2.5	0.2033	10.79
	3.0	0.2030	10.79
19.19	0.5	0.2029	15.52
	1.0	0.2029	13.80
	1.5	0.2020	12.88
	2.0	0.2025	12.88
	2.5	0.2024	12.87
	3.0	0.2023	12.94

Appendix Table A9 The influence concentration of phenol at various initial concentration for BC adsorption isotherm.

Replication	BC weight (g)	C_e (mg/L)	$\log C_e$	q_e	$\log q_e$	C_e/q_e
1	0.2032	2.94	0.468	0.128	-0.894	23.04
	0.2024	4.71	0.673	0.167	-0.776	28.10
	0.2021	7.64	0.883	0.324	-0.489	23.59
	0.2055	12.56	1.088	0.368	-0.434	33.31
	0.2023	15.21	1.182	0.491	-0.309	30.97
2	0.2011	2.91	0.465	0.132	-0.880	22.09
	0.2029	4.67	0.669	0.172	-0.766	27.21
	0.2024	7.64	0.883	0.324	-0.490	23.62
	0.2048	12.19	1.086	0.377	-0.423	32.30
	0.2025	15.15	1.181	0.499	-0.302	30.39
3	0.2030	2.94	0.468	0.128	-0.894	23.01
	0.2024	4.73	0.675	0.164	-0.784	28.77
	0.2046	7.67	0.884	0.317	-0.490	24.18
	0.2063	12.20	1.086	0.374	-0.427	32.61
	0.2022	15.15	1.181	0.499	-0.302	30.36
4	0.2022	2.90	0.463	0.132	-0.877	21.860
	0.2022	4.72	0.674	0.165	-0.782	28.57
	0.2033	7.66	0.884	0.321	-0.494	23.88
	0.2044	12.20	1.086	0.377	-0.423	32.31
	0.2022	15.15	1.181	0.499	-0.302	30.36

Appendix Table A10 The influence concentration of phenol at various initial concentration for BAC adsorption isotherm.

Replication	BC weight (g)	C_e (mg/L)	logC_e	q_e	logq_e	C_e/q_e
1	0.2072	2.88	0.459	0.133	-0.878	21.71
	0.2024	4.15	0.618	0.236	-0.628	17.62
	0.2021	6.42	0.807	0.476	-0.323	13.49
	0.2083	11.15	1.047	0.496	-0.305	22.51
	0.2025	12.88	1.110	0.778	-0.109	16.55
2	0.2011	2.79	0.446	0.147	-0.832	18.96
	0.2029	4.30	0.634	0.217	-0.664	19.82
	0.2024	6.42	0.807	0.476	-0.323	13.51
	0.2038	10.83	1.035	0.546	-0.263	19.86
	0.2024	12.88	1.110	0.779	-0.108	16.54
3	0.2020	2.79	0.446	0.147	-0.834	19.05
	0.2024	4.30	0.634	0.217	-0.663	19.78
	0.2086	6.63	0.821	0.436	-0.361	15.20
	0.2033	10.79	1.033	0.552	-0.258	19.54
	0.2023	12.87	1.110	0.781	-0.107	16.48
4	0.2021	2.80	0.447	0.146	-0.837	19.20
	0.2020	4.30	0.634	0.218	-0.662	19.74
	0.2023	6.43	0.808	0.474	-0.324	13.57
	0.2020	10.80	1.033	0.552	-0.258	19.55
	0.2024	12.94	1.112	0.771	-0.113	16.78

Appendix C

Calculation of dose, Cr(III) removal efficiency and adsorption capacity

1. Dose (g/L)

From the result in replication 1, the Cr(III) dose of BC was calculated.

The fifth result;

Carbon used	=	0.1018 g
Volume of Cr(III) solution	=	25.00 ml

$$Dose\ \left(\frac{g}{L}\right) = \frac{carbon\ used(g)}{volume\ of\ Cr(III)solution\ (ml)}\ x\ 1000$$

= (0.1018/25) x 1000

= 4.07 g/L

2. Cr(III) removal efficiency (E)

The removal efficiency (E) of adsorbent on Cr (III) was defined as

$$E(\%) = \left[\frac{C_0 - C_1}{C_0}\right] x100$$

Where C_o and C_1 are initial and final concentration of Cr solution (mg/L), respectively

From the result in replication 1, the Cr(III) removal efficiency of BC was calculated.

The first result;

Initial concentration of Cr(III) (C_0)	=	4.184 mg/L
Final concentration of Cr(III) (C_1)	=	2.110 mg/L

E (%) = ((4.184 – 2.110)/4.184) x 100

= 49 .57 %

3. Adsorption capacity (mg/g)

From the optimum dose of BC Adsorption capacity (mg/g) was calculated.

Initial concentration of Cr(III) (C_0)	=	4.184 mg/L
Final concentration of Cr(III) (C_1)	=	0.774 mg/L
Optimum dose	=	4.07 g/L

$$adsorption\ capacity = \frac{initial\ concentration\left(\frac{mg}{L}\right) - final\ concentration\ (\frac{mg}{L})}{dose\ (\frac{g}{L})}$$

= (4.184 – 0.774)/4.07

= 0.84 mg/g

Appendix D

Calculation of phenol value and specific surface area

1. Calculation of phenol value.

From the result in series 1, the phenol value of BC was calculate by AWWA B600.

The first result;

Carbon used = 0.2159 g

Initial concentration of phenol = 5.82 mg/L

Initial phenol volume = 25 ml

$$\% \text{ of residual filtrate normality } = \frac{residual\ phenol\ \left(\frac{mg}{L}\right) x\ 100}{phenol\ in\ test\ solution\ (\frac{mg}{L})}$$

= (2.1018 x 100)/5.82

= 36.01 %

% of adsorbed phenol (X) = 100 - % of residual filtrate normality

= 100 – 36.10

= 63.90 %

$$Carbon\ used\ (M) = \frac{1000\ x\ carbon\ weigh\ (g)}{phenol\ used\ (ml)}$$

= (1000 x 0.2159)/25

= 8.64 g/L

The next experiment was made like the first one but the amount of charcoal was increased until the phenol adsorption ability had higher than 90%. Then, the correlation between X/M and residual phenol (%) from all results as follow;

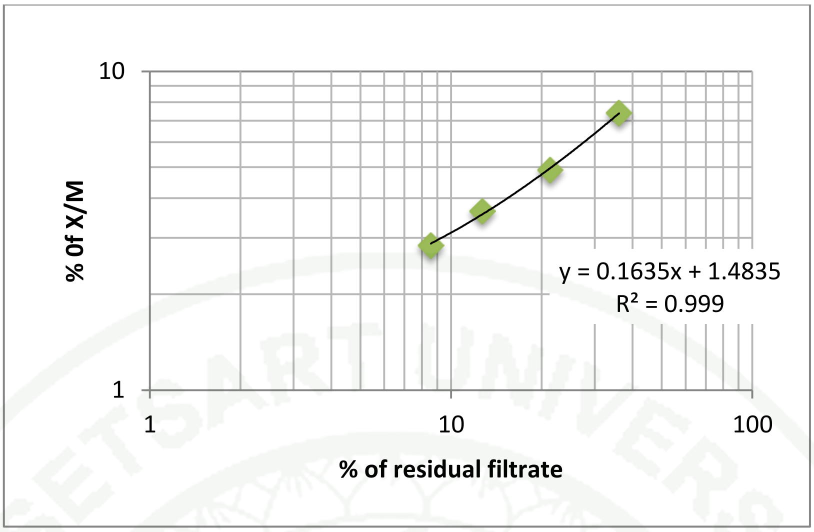

Appendix Figure D1 The relationship between X/M and residual phenol.

The X/M at 10% residual filtrate normality was calculated as follow;

$$y = 0.1635x + 1.4835$$

$$= 0.1635(10) + 1.4835$$

$$= 3.1185$$

Then, moisture was 2.55.

$$\text{Phenol value}\left(\frac{\text{mg}}{\text{L}}\right) = \frac{90}{\%\text{ of }\frac{\text{X}}{\text{M}}\text{ at 10\% residual filtrate normality}} \text{ x } \frac{100\% - \%\text{ of moisture}}{100}$$

$$\text{phenol value} = \frac{90}{3.1185} \text{ x } \frac{100 - 2.55}{100}$$

$$= 28.12 \text{ mg/L}$$

2. Calculate of specific surface area.

The specific surface area for adsorption of phenol onto BC was calculated by this equation; $S = \frac{Q_0}{MW} x\ Nx\ a$

Where;

S = the specific surface area (m^2/g)

Q_o = the the maximum surface coverage (formation of monolayer) of sorbent (mg/g)

MW = the molecular weight (g/mol) (for phenol = 94.11 g/mol)

N = the Avogadro number ($6.02x10^{23}$ molecule/mol)

a = the cross sectional area of adsorbate ($Å^2$) (for phenol = 52.2 $Å^2$)

For example, the specific surface area for adsorption of phenol onto BC was calculate as follow;

Q_0 = 1.54 mg/g

MW = 94.11 g/mol

N = 6.02x1023 molecule/mol

a = 52.2$Å^2$

$$S = \frac{1.54\ x\ 10^{-3}}{94.11}\ x\ (6.02\ x\ 10^{23}) x\ 52.2\ x\ 10^{-20}$$

S = 5.14 m^2/g

Therefore, the specific surface area for adsorption of phenol onto BC was 5.14 m^2/g.

CURRICULUM VITAE

NAME : Miss Chittraporn Chantasorn

BIRTH DATE : March 18, 1985

BIRTH PLACE : Chiang Rai, Thailand

EDUCATION :

YEAR	**INSTITUTION**	**DEGREE/DIPLOMA**
2007	Kasetsart University	B.Sc. (Chemistry)

POSITION/TITLE : Graduates student

WORKPLACE : Faculty of Science, Kasetsart University

SCHOLARSHIP : Center for Innovation in Chemistry: Postgraduate Education and Research Program in Chemistry (PERCH-CIC)) Science and Technology Postgraduate Education and Research Development Office (PERDO) 2007-2009.